ENHANCED TRAILER BACKING

By

AMIT DAVID JAYAKARAN

A THESIS PRESENTED TO THE GRADUATE SCHOOL
OF THE UNIVERSITY OF FLORIDA IN PARTIAL FULFILLMENT
OF THE REQUIREMENTS FOR THE DEGREE OF
MASTER OF SCIENCE

UNIVERSITY OF FLORIDA

2004

This document is dedicated to my parents.

ACKNOWLEDGMENTS

I would like to express my gratitude to Dr. Carl Crane III, who as my advisor came up with the idea for this thesis and who guided me for the past year and a half. I would also like to thank Dr. David Dooner for his immense help in getting my work started and putting me on the right track. I would also like to thank Dr. Robert Bicker who helped me through the last part of my work. I would like to thank Dr. John Kenneth Schueller for being on my committee.

I also owe a lot of gratitude towards Shannon Ridgeway and Dr. Carol Chesney who helped me at various points during my work.

On a more personal note I would like to thank my parents and brother for their love and support. I would also like to thank my friends at the University of Florida who have directly and indirectly contributed to my work here.

TABLE OF CONTENTS

LIST OF TABLES

LIST OF FIGURES

Abstract of Thesis Presented to the Graduate School
of the University of Florida in Partial Fulfillment of the
Requirements for the Degree of Master of Science

ENHANCED TRAILER BACKING

By

Amit David Jayakaran

May 2004

Chair: Carl D. Crane III
Major Department: Mechanical and Aerospace Engineering

In many instances, an autonomous vehicle has a trailer attached to it. The trailer readily follows the vehicle's path of motion while it moves forward. However, when the vehicle reverses, for example to correct its path or to get out of a tight corner, the trailer has a tendency to jackknife.

This thesis deals with several approaches to solve this problem, none of which requires any modification to the vehicle steering control itself. The approach dealt with in detail involves actually moving the point that couples the trailer to the vehicle. Depending on the instant center of rotation of the vehicle with respect to the ground, changes are made in the position of the coupling point to modify the instant center of the trailer with respect to ground in such a manner as to maintain stability during backing. The results obtained are verified in both a computer simulation and a physical model. The results were found to be excellent with the vehicle being able to back up with the trailer through any distance at moderate speeds.

CHAPTER 1
INTRODUCTION

When a vehicle backs up with a trailer attached the trailer never seems to follow the path it is expected to. Drivers with a lot of driving experience can even be often confused by an uncooperative trailer while backing. It takes a lot of experience to be able to back up a trailer. For an autonomous vehicle with a trailer, backing with a trailer is a really big challenge as it places additional constraints on the system's path of travel.

Jackknifing is defined as the condition when a trailer bends or folds up on the vehicle pulling it, similar to a jackknife shown in Figure 1-1. As far as backing up with a trailer most work done so far involves increasing the number of constraints on the vehicle in order to prevent jackknifing which thereby reduces the probability of the vehicle following a defined path closely. Basically most algorithms will end up causing the vehicle to make extra or at least wider turns. This may in some cases be unacceptable.

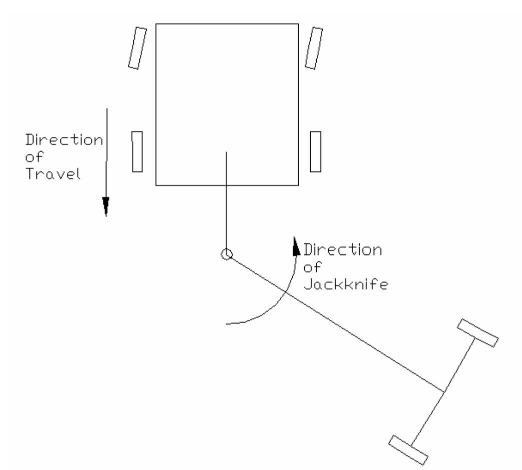

Figure 1-1: Jackknifing

The following thesis deals with different approaches to prevent jackknifing without having to place any extra constraints on the vehicle. It aides the autonomous vehicle to back up with a trailer as if it were not there at all. This basically means all that is needed to do is to place the necessary sensors on any vehicle and it will be able to back up without having to change anything on the vehicle. The design of this system enables it to be transferred to a regular vehicle attached to a trailer, thus aiding a human in backing a trailer.

Jackknifing is chiefly caused due to incorrect backing of a vehicle with a trailer. Jackknifing can also be caused during forward motion when the vehicle brakes suddenly and the trailer continues to move and since it can’t move forward it swings sideways and jackknives. However this thesis will deal with jackknifing caused due to backing only. Such a system is of particular interest for an autonomous vehicle. Many autonomous vehicles carry their surveillance equipment in a trailer and so the path that the trailer follows is very important. Besides this sometimes the vehicle may find itself in a tight corner or some situation in which it may need to back up a particular distance, causing it to jackknife.

The vehicle is nonholonomic because of its rolling constraints. The configuration of the vehicle is given by two position coordinates and an angle and there are only two inputs, linear and angular velocity. Thus the system has two degrees of freedom. For every trailer that is added, the configuration of the vehicle depends on one more constraint that is the angle between the trailer and what it is attached to.

Thesis Organization

The following thesis is divided into five chapters.

The second chapter, Review of Literature, deals with the literature review and past work done in this area.

The third chapter, Approach, involves a look at the different approaches that can be used to solve the given problem. It lists the assumptions made during the entire analysis and derives the equations required for the analysis and implementation of the model.

The fourth chapter, Design Description gives a description of the computer model and then the physical model that was built based on chapter three.

The fifth chapter, Results and Conclusions, describes the results that are obtained and also the future work that is possible in this area.

CHAPTER 2
REVIEW OF LITERATURE

Overview

In the past much work has been done on stabilizing trailers during their forward motion for different speeds, especially high speeds. For example Tesar and Matthew [1] discuss a four bar mechanism that helps eliminate swaying at high speeds.

Most work in path planning of a vehicle with a trailer has been done by introduction of additional constraints on the system [2-7]. A vehicle already has nonholonomic constraints and the introduction of additional constraints further restricts the path the vehicle is able to take. The work done on Hilare and its trailer [5] outlines several equations for backing up with a trailer with and without off-hooking. These approaches though successful, reduce the efficiency of path planning because of the introduction of additional constraints.

The backing up of a vehicle trailer system can be compared to that of an inverted pendulum. In an inverted pendulum the system is stable only in only one position [8-9]. In order to stabilize the inverted pendulum it is moved horizontally to ensure that that it always remains vertical. With a trailer system too this is partly true. However the stable point keeps changing depending on the wheel angle, because for different wheel angles the trailer chooses another stable angle.

To further facilitate the understanding of some of the terms used in this thesis some terms are defined below.

Definitions

Jack Knifing

Jackknifing is defined as the condition when a trailer bends or folds up on the vehicle pulling it, similar to a jackknife.

Instant Center of Rotation

Instant Center of Rotation is defined as the imaginary point about which the vehicle appears to be turning with respect to ground. The instant center of rotation is at infinity when the vehicle is moving straight. It is located at the center of the minimum turning radius of the vehicle when the vehicle is making the sharpest possible turn it can make.

Ackerman steering is typically used in steered wheeled vehicles so that the instant center is located at the point at which the perpendiculars from all the wheels meet. As long as these lines meet at only one point the system is stable. Vehicle manufacturers make sure these lines meet at the designated point when turning. Figure 1 shows the instant center of rotation for a wheeled vehicle with Ackerman steering.

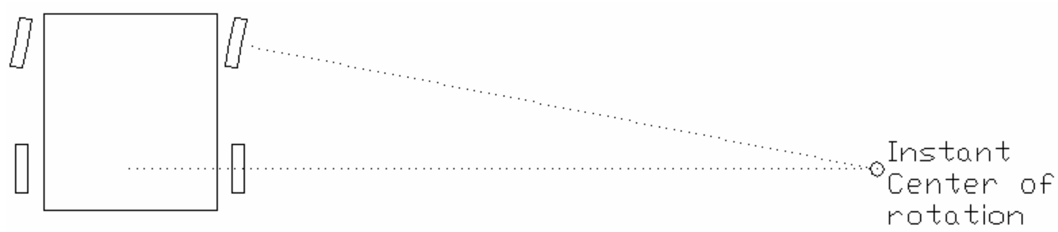

Figure 2-1: Instant Center of Rotation

Radius of Turn

Radius of Turn is the distance between the instant center of rotation and the center of the rear axle of a front wheel steered vehicle.

Curvature of Path

The inverse of the radius of turn is called the curvature. Only in the case that the vehicle is a two wheel system is it possible for it to follow a curvature of infinity.

Nonholonomic Constraints

Nonholonomic constraints arise from the fact that the wheels of a four wheeled vehicle can only roll or spin on the ground but allow for no slide sideways [2]. For instance a vehicle has two controls – linear and angular velocities. However this vehicle moves in a three dimensional configuration space. As a result, all paths on a configuration space are not feasible. To add to this, when there is a trailer it further reduces the possibilities. For example, if a vehicle has to back up straight it can do so without a problem if there is no trailer. But when a trailer is attached it will have to steer gently right and left continuously in order to make sure the trailer doesn't jackknife. This becomes tougher when negotiating a turn as the vehicle has to now make a turn in the opposite direction first to align the trailer in the direction the trailer has to go and then only start negotiating the turn. This can be more clearly seen by observing a person backing up with a trailer. This thesis outlines a method by which some constraints on the system associated with the trailer may be eliminated [3]. Nonholonomic equations are characterized by constraint equations involving the time derivatives of the system configuration variables. These equations are non integrable; they typically arise when the system has less control than the configuration variables. The rolling contact of the wheels with the surface it moves on is what essentially gives rise to nonholonomic motion [10-11]

Small Time Controllable

Small-time controllability means that the set of configurations reachable after any given time always contains a neighborhood of the starting configuration. As a consequence any collision free path can be approximated by a sequence of collision free feasible configurations [5].

Off-Hooking

Off-hooking is when the trailer is hooked at a distance from the rear axle of the vehicle.

Center of Rotation

The center of rotation is defined as the point of rotation of the trailer with respect to the vehicle. It is usually the point at which the trailer is attached to the vehicle.

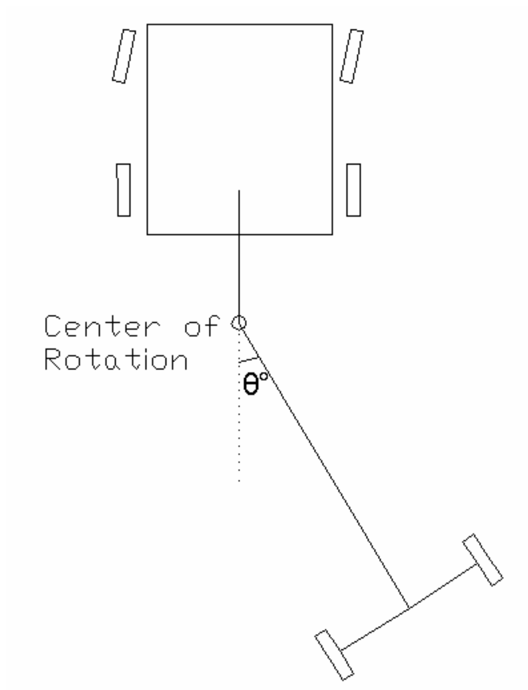

Figure 2-2: Center of rotation

CHAPTER 3
APPROACH

Assumptions

The following assumptions about the system are presented:

- It is assumed that the contact between the ground and each every wheel is pure rolling contact
- All the systems are planar.

Approach

When a trailer is attached to the system, there is one more factor that is now contributing to the instant center of rotation. When this vehicle moves forward the trailer follows the vehicle and will negotiate turns without any problems. As shown later the trailer naturally tries to align itself with the instant center of rotation of the vehicle by rotating about its center of rotation at the hinge. The trailer being aligned with the instant center of rotation of the vehicle simply means that the line through the trailer axle passes through the instant center of rotation of the vehicle. However, when backing up the vehicle with the trailer, the system is as unstable as trying to balance an inverted broom on one's hand. There are only two positions at which the trailer will be stable and out of these two positions, as shown later only one really is feasible. What makes this problem worse is that this position of stability changes as the steering angle of the vehicle changes. Thus if it can be somehow ensured that the line through the wheel axle of the trailer passes through the instant center of rotation of the vehicle, the system will be stable. In other words, if the instant center of the trailer with respect to ground is always coincident with the instant center of the vehicle with respect to ground, then the vehicle and trailer can travel in reverse in a stable manner. This condition is shown in Figure 3-1 and 3-2.

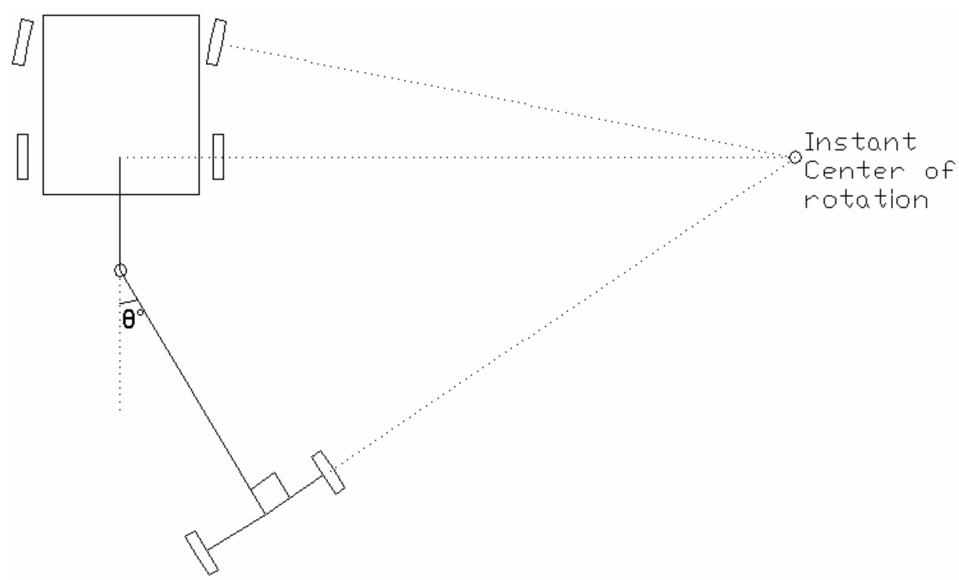

Figure 3-1: Combined Instant Center

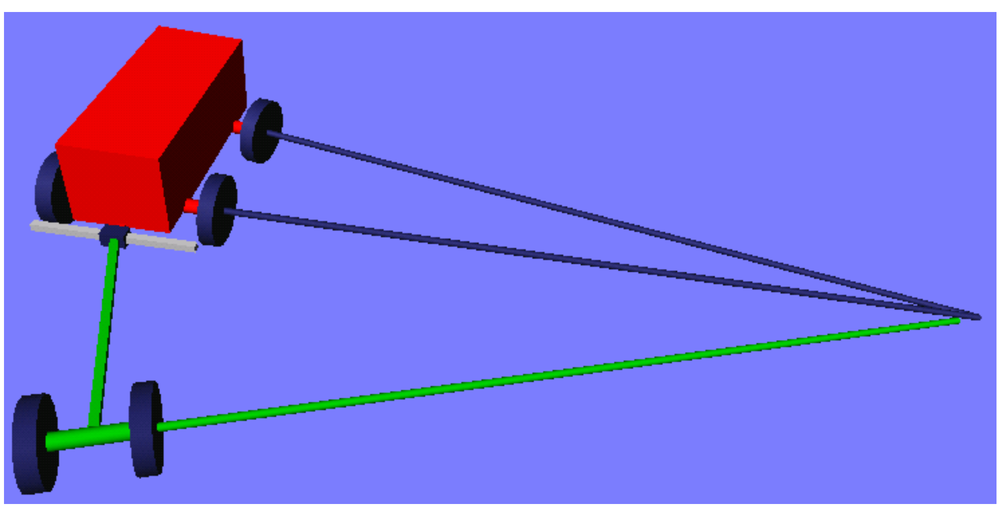

Figure 3-2: Combined Instant Center

This thesis outlines alternative methods for coupling between the vehicle and the trailer to ensure that the instant center of rotation is always the same for the vehicle as well as the vehicle trailer system. It also describes in detail a generic system that can be extended to any vehicle-trailer system in the market.

The trailer angle corresponding to different steering angles can be calculated by many methods. Below are outlines of some of the methods that have been used in this thesis to cross verify results.

The above system is simplified into a geometric system and is represented in Figure 3-3. The values for 'd', the distance of the trailer hitch from the rear axle of the vehicle, '*l*', the distance from the trailer hitch to the trailer wheel axle, and 'a' the distance between the instant center point and the center of the vehicle's rear axle, are assumed to be known.

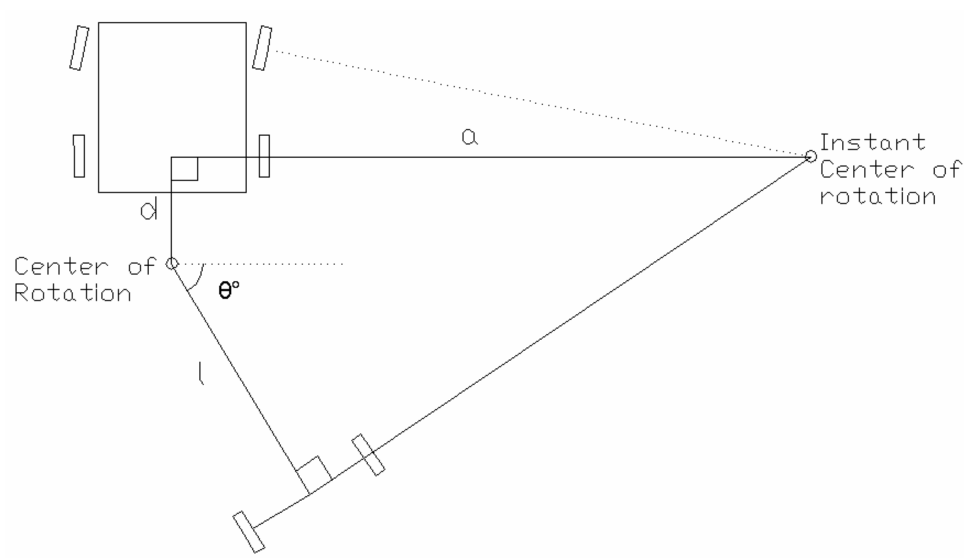

Figure 3-3: Simplified system and the solution polygon

It is found that there are two possible solutions for the angle θ, the angle between the line along the trailer and the line along the vehicle's rear axle, for this system. These solutions are show in the Figures 3-4 and 3-5 below.

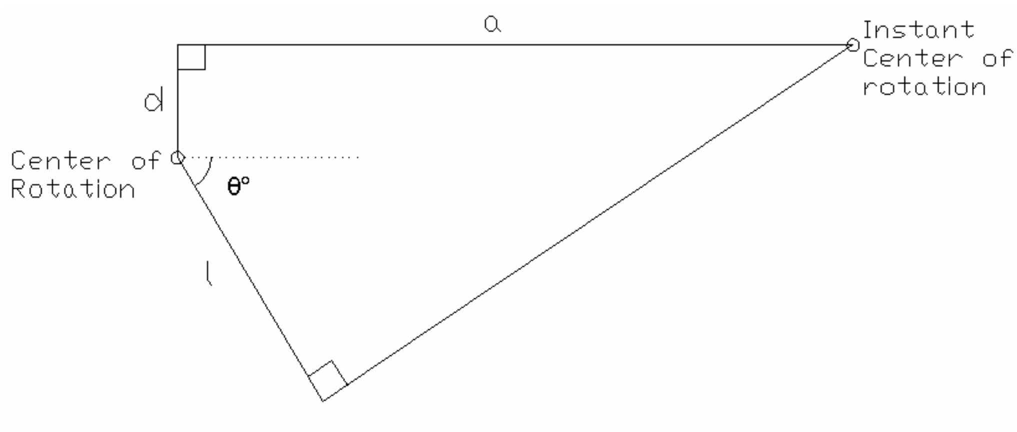

Figure 3-4: Solution 1 for the Angle θ

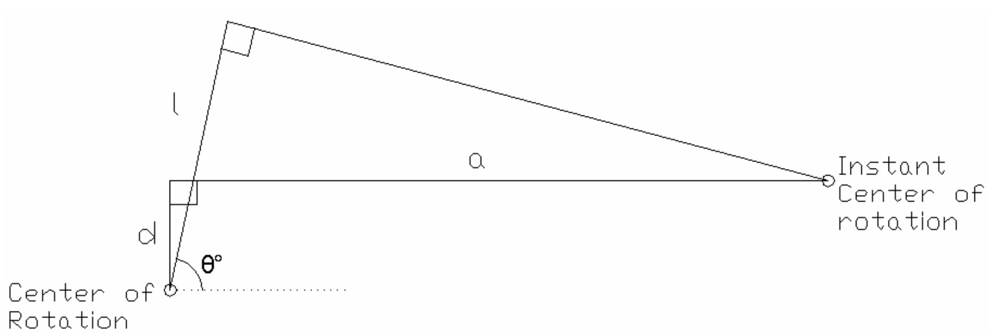

Figure 3-5: Solution 2 for the Angle θ

Obviously the first solution is the only one of interest because the second solution would represent an existing case of jackknifing. The interesting point about the second solution is that in this condition the trailer is apparently being pulled when the vehicle travels in reverse. As a result it will naturally align itself to achieve the angle to coincide with the instant center of rotation. A method to find the value for θ for a given value of the steering angle ϕ (shown in Figure 3-6) that will keep the trailer stable while backing, i.e. the value of θ that will cause the line along the trailer axle pass through the instant center of rotation of the vehicle, will be presented in the next section. After deriving the stable position of the trailer different methods to keep the trailer stable at those positions will be discussed.

Stable Values of θ

Analytical Solution for the Polygon

The analytical method involves converting the system into a polygon and finding the various solutions that satisfy it. The polygon is shown in Figure 3-7. The aim is to find a solution to the angle θ in relation to 'a', the distance of the instant center from the center of the rear axle. The distance of the instant center is calculated from the wheel angle (ϕ), the width of the vehicle (w) and the distance between the rear and front axles (L_1).

The distance of the instant center (i) from the rear wheel is given by

$$i = L_1 \times \tan\left(\frac{\pi}{2} - \Phi\right) \tag{3.1}$$

Now the term of interest in is 'a', the distance between the center of the axle and the instant center which is given by

$$a = \frac{w}{2} + i \tag{3.2}$$

Once this is determined, the parameters for the polygon are calculated. The terms x, y, and z are defined as shown in Figure 3-7.

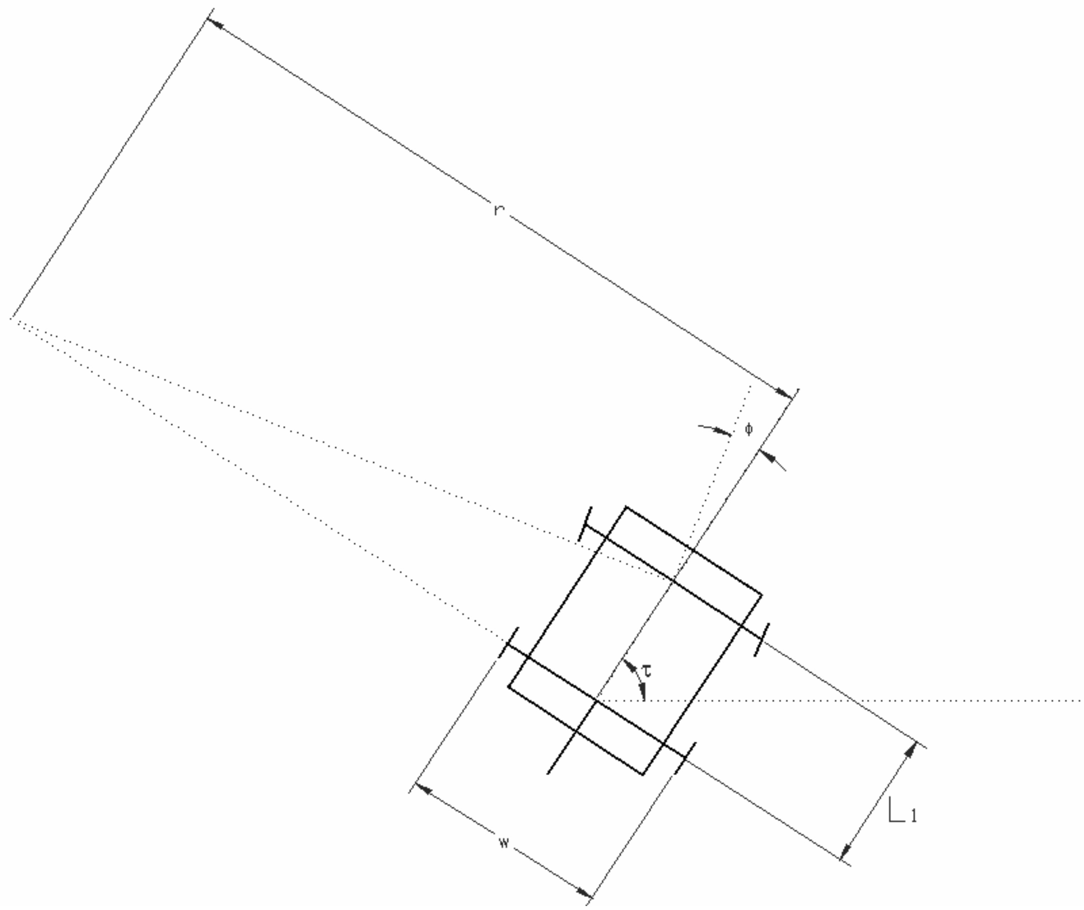

Figure 3-6: Calculation of the Distance of the Instant Center from the Center of the Rear Axle

Figure 3-7 shows the trailer and the vehicle polygon. The distances x and y can be written in terms of the trailer rotation angle θ as

$$x = \frac{d}{\cos\theta} \tag{3.3}$$

$$y = d \tan\theta \tag{3.4}$$

From the outer triangle of Figure 3-7 which has sides of length z, a+y, and *l*+x it is apparent that

$$\cos\left(\frac{\pi}{2} - \theta\right) = \frac{l + x}{a + y} \tag{3.5}$$

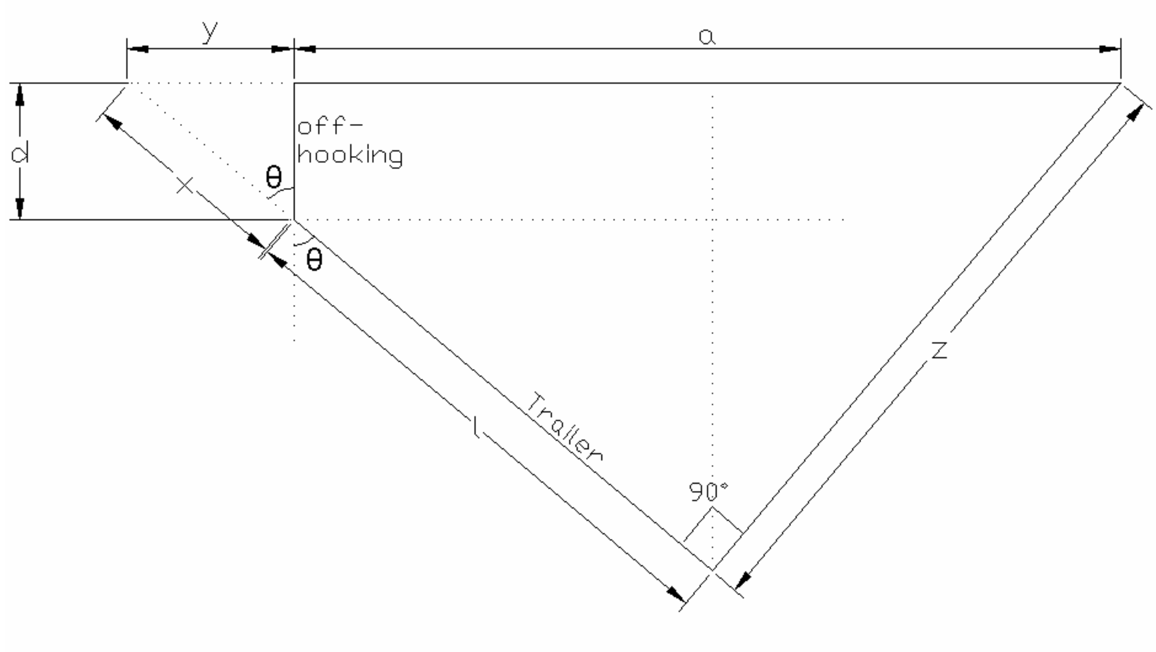

Figure 3-7: Trailer and Vehicle Polygon

From equations (3.3), (3.4) and (3.5) the following expression can be written

$$\cos\left(\frac{\pi}{2}-\theta\right)=\frac{l+\dfrac{d}{\cos(\theta)}}{a+d\tan(\theta)} \tag{3.6}$$

This equation relates the trailer angle, θ, to the instant center distance, a. The left side of (3.6) will equal $\sin\theta$. Making this substitution and multiplying both sides by $(a+d\tan\theta)$ gives

$$\sin\theta\cos\theta(a+d\tan\theta)=l+\frac{d}{\cos\theta} \tag{3.7}$$

Multiplying throughout by $\cos\theta$ gives

$$\sin\theta\cos\theta(a+d\tan\theta)=l\cos\theta+d \tag{3.8}$$

Substituting $\tan\theta=\dfrac{\sin\theta}{\cos\theta}$ and regrouping gives

$$a(\sin\theta\cos\theta)+d(\sin^2\theta-1)-l\cos\theta=0 \tag{3.9}$$

Substituting $(\sin^2\theta-1)=-\cos^2\theta$ and dividing throughout by $\cos\theta$ gives

$$a\sin\theta-d\cos\theta-l=0 \tag{3.10}$$

Two values of θ will satisfy this equation for each given value of a. One of these values will be physically realizable as shown in Figures 3-4 and 3-5.

There are two methods of solving this equation [12]. Rewriting the above equation as

$$A\cos\theta+B\sin\theta+D=0 \tag{3.11}$$

where

$$A=-d, B=a, D=-l$$

Trigonometric Solution

This technique begins by dividing (3.11) by $\sqrt{A^2+B^2}$ to yield

$$\frac{A}{\sqrt{A^2+B^2}}\cos\theta+\frac{B}{\sqrt{A^2+B^2}}\sin\theta+\frac{D}{\sqrt{A^2+B^2}}=0 \tag{3.12}$$

Using the right-angled triangle shown in Figure 3-8 it is possible to substitute

$$\frac{B}{\sqrt{A^2+B^2}}=\sin\gamma \tag{3.13}$$

$$\frac{A}{\sqrt{A^2+B^2}}=\cos\gamma \tag{3.14}$$

Because the sine and cosine of γ are expressed in terms of all known quantities, a unique value for the angle γ can be obtained. Substituting (3.13) and (3.14) into (3.12) gives

$$\cos\gamma\cos\theta + \sin\gamma\sin\theta + \frac{D}{\sqrt{A^2 + B^2}} = 0 \tag{3.15}$$

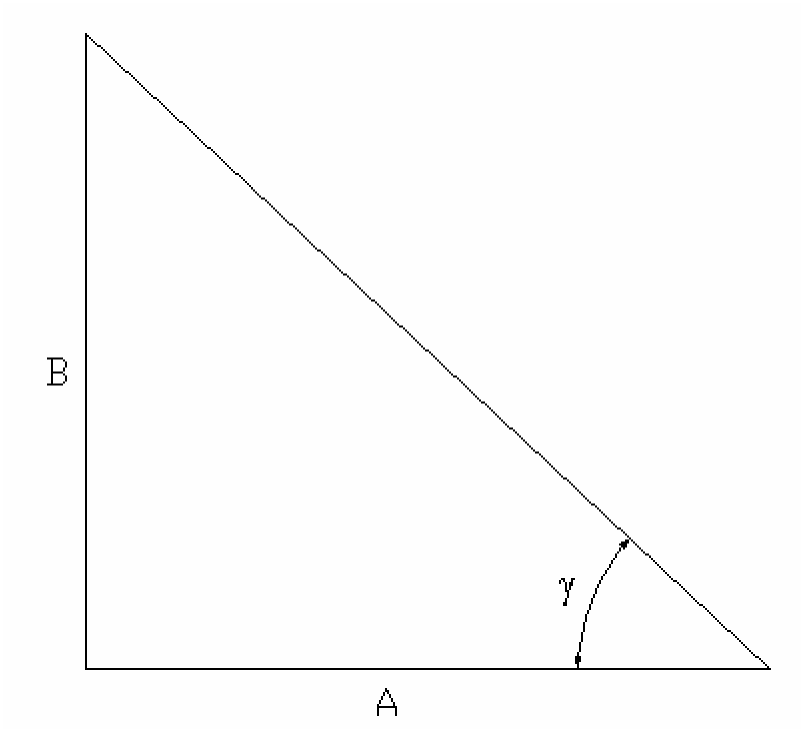

Figure 3-8: Triangle to Help Simplify the Solution

Using the trigonometric identity

$$\cos(\alpha - \beta) = \cos\alpha\cos\beta + \sin\alpha\sin\beta \tag{3.16}$$

Putting (3.16) into (3.15) and regrouping gives

$$\cos(\theta - \gamma) = \frac{-D}{\sqrt{A^2 + B^2}} \tag{3.17}$$

Thus there are two values for the quantity $(\theta - \gamma)$ because the cosine yields two values in the range $0 \le \theta \le 2\pi$. But since γ is unique two value of θ can now be obtained.

The Simulink Model

A Simulink model was built based on the results discussed above to plot the desired values of the trailer angle with respect to the steering angle of the vehicle. This is a component of the main program sued to make a computer model of the complete system described in more detail in the Appendix.

Figure 3-10 illustrates the base model. It takes the vehicle constants namely, vehicle width, distance of trailer hitch (off-hooking), length of trailer, and distance of rear and front axles (wheel base) as the input. The steering angle is simulated with a ramp that runs from 0 to 70 degrees. The system is symmetric and so the same conclusions can be deduced from the -70 to 0 degree range. Figure 3-11 and Figure 3-12 are for reading constants from the user and making them globally available. Figure 3-13 and 3-14 calculate constants that are required during the simulation. The results of these blocks are fed into a Matlab function that outputs the θ values that are stable, i.e., the values of θ that will cause the line through the trailer axle to pass through the vehicle's instant center point. The results are then plotted to view the response of the steering angle on trailer position.

The various parameters were set as

- Distance between the front and rear axles = 1.5 m
- Width of the vehicle = 1 m
- Distance of hinge from the rear axle = 0.3 m
- Length of the trailer = 1 m

The output is in the form of the two possible solutions of theta. The results were viewed on a virtual scope and are shown in Figures 3-14 and 3-15. Besides this the turning radius is also shown in Figure 3-16.

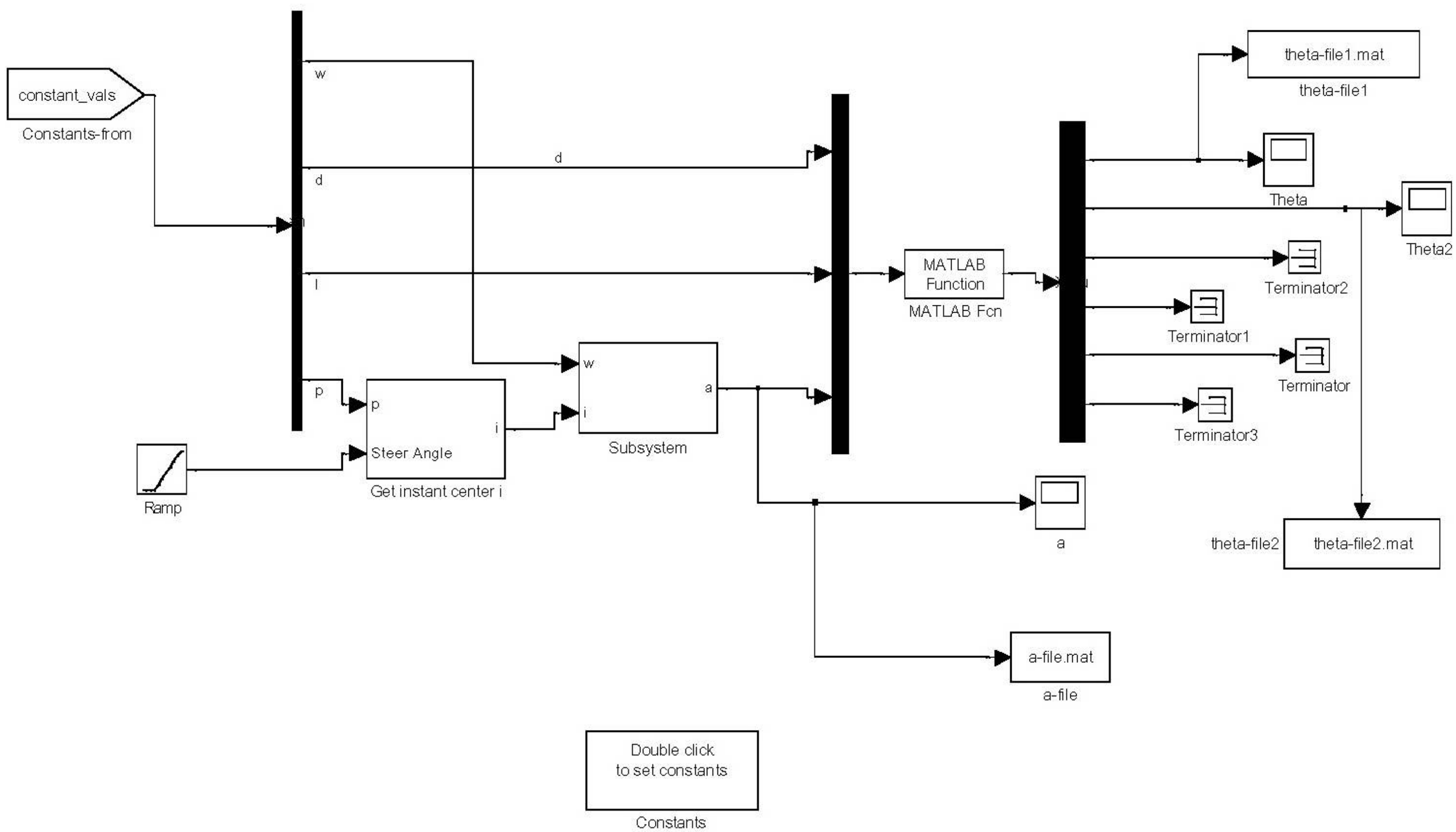

Figure 3-9: Base Model for θ Calculation

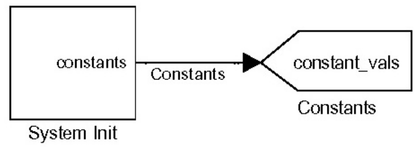

Figure 3-10: Reading Constants - I

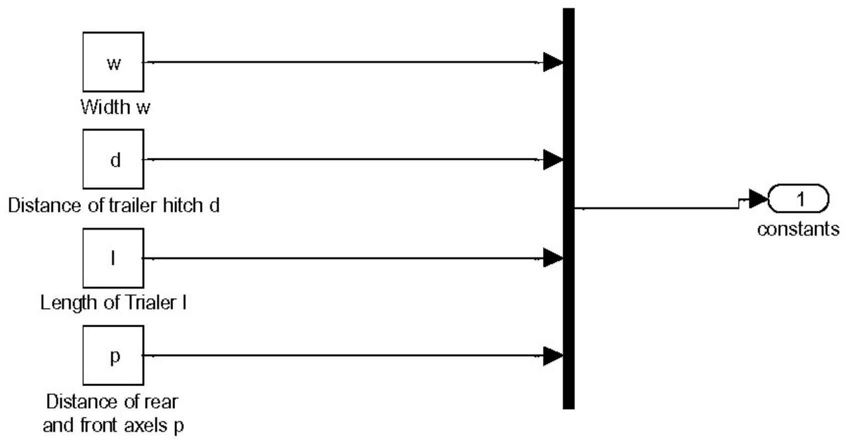

Figure 3-11: Reading Constants - II

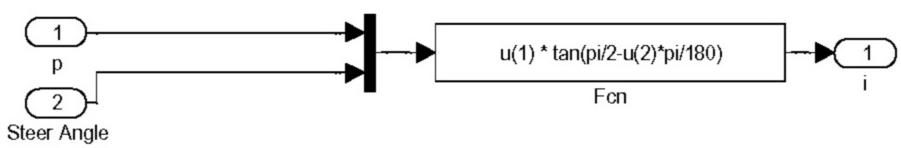

Figure 3-12: Calculation of the Instant Center - I

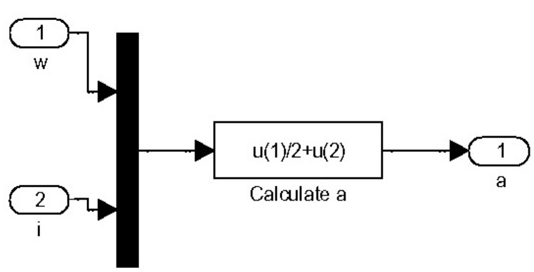

Figure 3-13: Calculation of the Instant Center - II

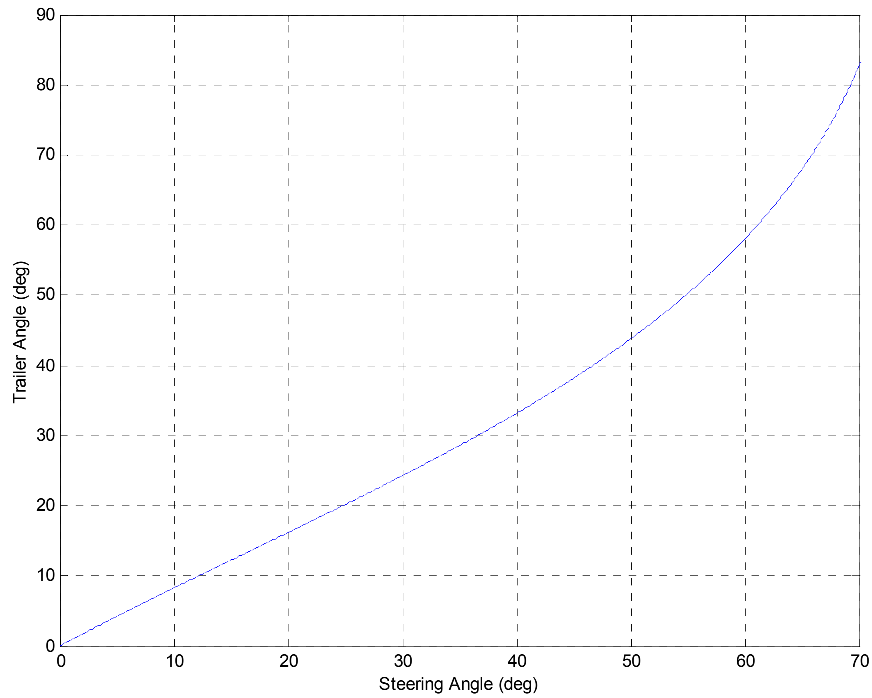

Figure 3-14 Solution for First Theta Value

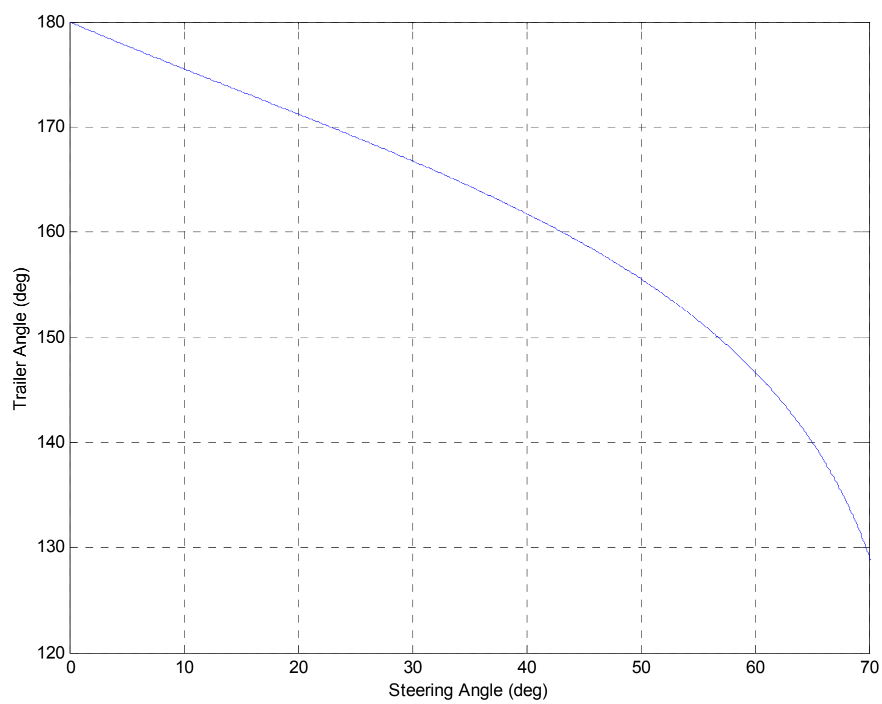

Figure 3-15 Solution for Second Theta Value

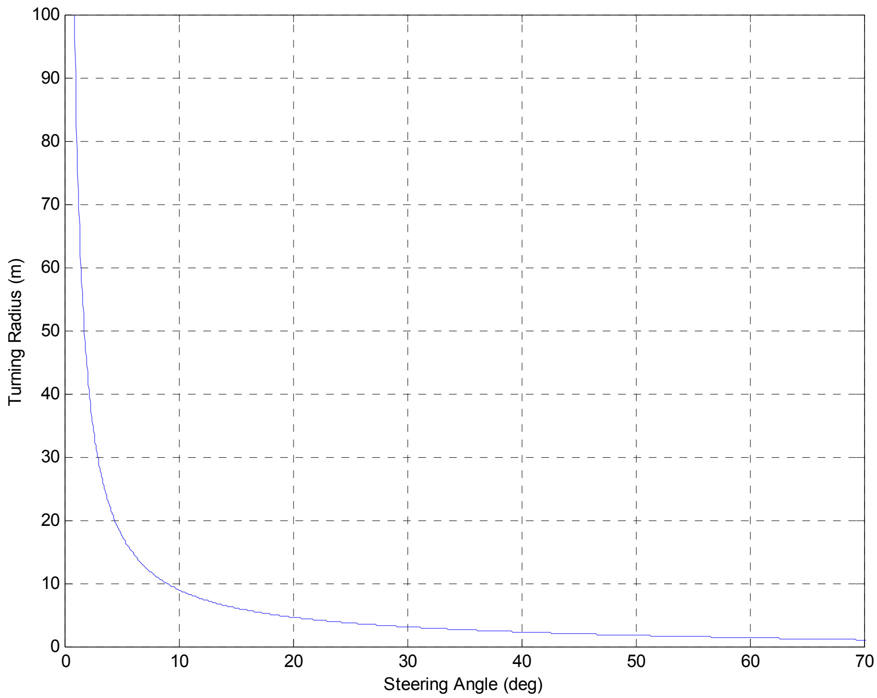

Figure 3-16: Plot of Turning Radius

Velocity Analysis

So far all calculations are done not considering the vehicle motion at all. Thus in order to verify these results a velocity analysis is performed. The velocity analysis will result in a relation between the trailer angle, change in the trailer angle and the velocity of the vehicle. Now in this relation the change in trailer angle is set to zero as this is what is desired at steady state. If the relation is similar to those obtained earlier then the above results are verified.

Let the vehicle be moving at a velocity of v and the average wheel turning angle be ϕ. Both wheels are usually at almost the same angle and both contribute to the radius of turn. In order to consider both their contributions the average is taken.

The following information is assumed to be given:

- the wheel base of the vehicle is L_1
- the amount of off-hooking is l_r
- The length of the trailer l_t

The following notation is introduced:

- Orientation of the vehicle with the x axis τ
- Angle between the vehicle and the trailer θ
- Turning radius a

The setup is shown in Figure 3-17.

The angular velocity of the vehicle about its instant center of rotation is given by,

$$\omega = \frac{v}{a} \tag{3.18}$$

Now,

$$\tan\phi = \frac{L_1}{a} \tag{3.19}$$

Rewriting,

$$a = \frac{L_1}{\tan\phi} \tag{3.20}$$

From (3.20) and (3.18)

$$\omega = \frac{v\tan\phi}{L_1} \tag{3.21}$$

The omega is now translated to the center of the rear axle [13-18]. This leaves an angular velocity of ω about the center of the rear axle and a velocity v as shown in Figure 3-18. Thus the linear velocity of the center point of the rear axle is a counter clockwise ω and a velocity v in the direction of the front wheels.

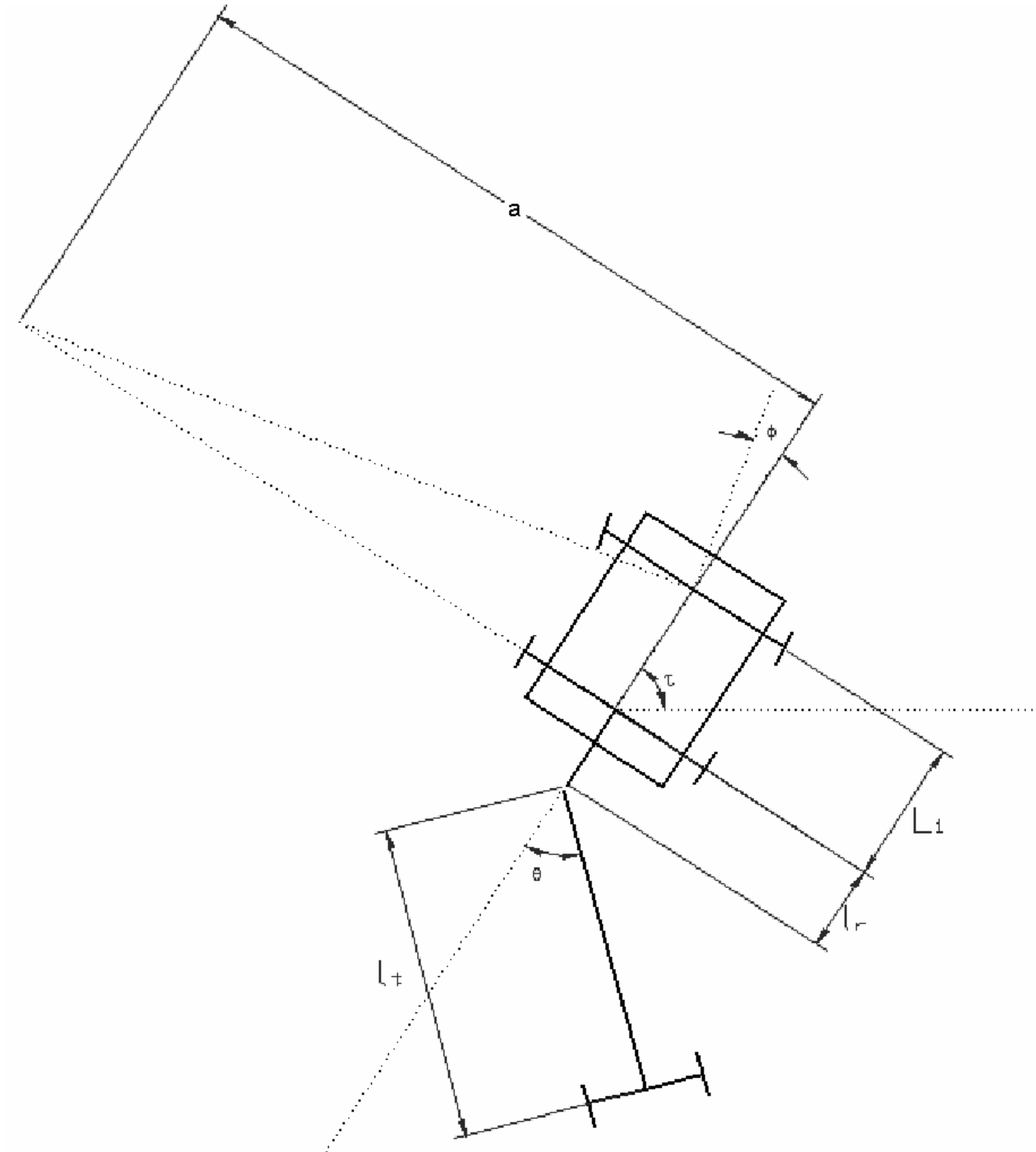

Figure 3-17: The Setup for the Slider Analysis

Now it is known that

$$_G\theta_T = {}_G\theta_V + {}_V\theta_T \tag{3.22}$$

Differentiating (3.22)

$$_G\dot{\theta}_T = {}_G\dot{\theta}_V + {}_V\dot{\theta}_T \tag{3.23}$$

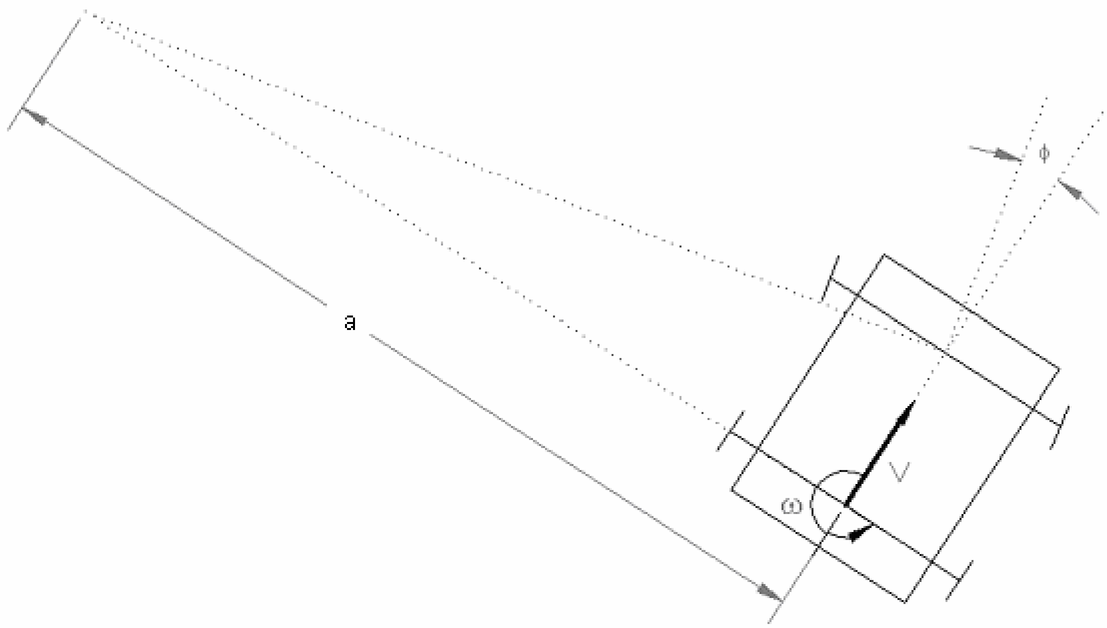

Figure 3-18: Closer Look at the Velocity Setup at the End of the Trailer

It is required to find ${}_V\dot{\theta}_T$,

$${}_V\dot{\theta}_T = {}_G\dot{\theta}_V - {}_G\dot{\theta}_T \tag{3.24}$$

It is known that

$${}_G\dot{\theta}_V = -\omega \tag{3.25}$$

The negative sign is put there because ω is counter clockwise.

The velocity at the hinge has two components. One is from the velocity v of the vehicle and the other caused due to the angular velocity, ω, of the vehicle. The velocity v is at an angle of τ to the x-axis. The velocity caused due to ω ($l_r\omega$) is perpendicular to the off hooking.

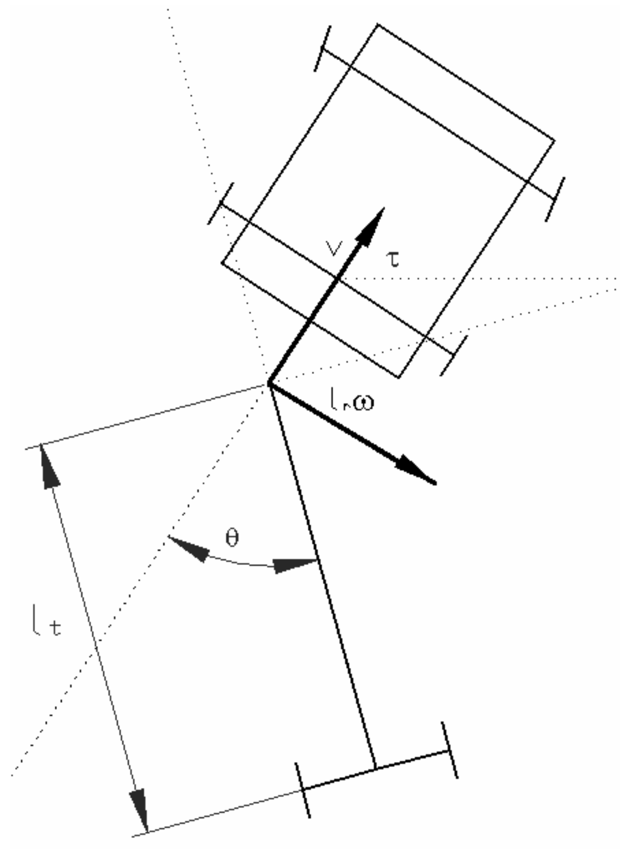

Figure 3-19: Velocities at the Trailer

The component of the velocity that causes the trailer to rotate about the center point of its axle is

$$\omega l_r \cos\theta + v\cos\left(\frac{\pi}{2} - \theta\right) \ . \tag{3.26}$$

Thus the angular velocity of the trailer is

$${}_G\dot{\theta}_T = \frac{\omega l_r}{l_t}\cos\theta + \frac{v}{l_t}\sin\theta \ . \tag{3.27}$$

Substituting (3.27) and (3.25) into (3.24) gives

$${}_V\dot{\theta}_T = -\omega - \frac{\omega l_r}{l_t}\cos\theta - \frac{v}{l_t}\sin\theta \ . \tag{3.28}$$

This equation is the control equation. By finding values to push ${}_V\dot{\theta}_T$ to zero when in steady state, the trailer can be made stable during backing.

The correct value of θ is obtained when ${}_V\dot{\theta}_T = 0$. Thus (3.28) reduces to

$$-\omega - \frac{\omega l_r}{l_t}\cos\theta - \frac{v}{l_t}\sin\theta = 0 \tag{3.29}$$

Dividing throughout by v and substituting equation (3.18) into (3.29) gives

$$-\frac{1}{a} - \frac{l_r}{a l_t}\cos\theta - \frac{1}{l_t}\sin\theta = 0 \tag{3.30}$$

$$l_t + l_r\cos\theta + a\sin\theta = 0 \tag{3.31}$$

It is seen that this equation is equivalent to equation (3.48), thus verifying the results. Another interesting fact is that the desired trailer angle is independent of the vehicle speed when the system is at a stable condition. Thus most calculations for stable conditions can be done without knowledge of the velocity of the vehicle.

Stabilizing the Trailer

Stabilizing the trailer involves trying to change θ to the desired angle. This boils down to a control problem where orientation of the trailer is being controlled with just one control parameter. There are several approaches of doing this.

One approach that is relatively simple to implement is to place a motor at the hinge point and force the trailer to take the angle that is calculated from above. This approach is of course feasible only in cases where the trailer weight is very low and where the vehicle doesn't steer unless it is in motion. There will be very high levels of slippage when the trailer is being forced to an angle but once it achieves the correct desired angle, there will be little to no slippage.

Another approach involves placing a non linear gear train between the steering and the trailer. This way whenever the vehicle is steering, the trailer gets appropriately steered too. This is similar to the above approach except that the link is now mechanical and not electrical. Besides the disadvantages stated above this approach also has the added disadvantage of the increased steering force required.

Slider

In all the above approaches the trailer is pushed to a particular position which is stable. Thus in these cases the ideal trailer angle is known. Another method would be to slide the hinge of the trailer along the back of the vehicle to such an extent so as to rotate the trailer to the desired trailer angle. This can be done by means of placing a slider on the back of the trailer as seen in Figure 3-17. As the trailer angle changes the slider moves to compensate it.

Now from reproducing equation (3.28)

$$_V\dot{\theta}_T = -\omega - \frac{\omega l_r}{l_t}\cos\theta - \frac{v}{l_t}\sin\theta \tag{3.32}$$

From the above equation it is seen that the only term that will be affected when the slider moves is the v term corresponding to the velocity of the vehicle at the hinge. v was earlier calculated as

$$v = r\omega \tag{3.33}$$

Now it will be given by

$$v = (r + x)\omega \tag{3.34}$$

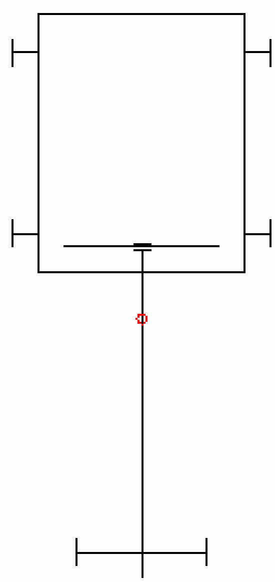

Figure 3-20: Slider Setup.

Thus using equation (3.34) in (3.32) the required results are obtained. However usually for reasonable turning angles x will be very small compared to r and so it can be ignored. So for all practical purposes the results obtained in equation (3.28) are sufficient.

A method of implementation of this control system is discussed in Chapter 4.

CHAPTER 4
DESIGN DESCRIPTION

Mechanisms to Align Trailer

The objective, as stated in the previous chapter is to obtain stable backing of the vehicle and trailer by causing the angle θ to be at such a value that the line along the trailer axle will pass through the instant center point of the vehicle during the backing maneuver. Two approaches will be presented that force the trailer to remain properly aligned as the vehicle is driven in reverse. A physical model to test the approaches is then described. Results of tests with the physical model are presented in Chapter 5. Equation (3.31) is being repeated here as (4.1)

$$l_t + l_r \cos\theta + a \sin\theta = 0 \tag{4.1}$$

Method I

The simplest most straight forward method of ensuring that the system is stable is to always ensure that the trailer angle satisfies the above equation. In this case all that needs to be done is to ensure that the Equation (4.1) is satisfied and if it not the slider is moved such that it is. This is shown in Figure 4-1.

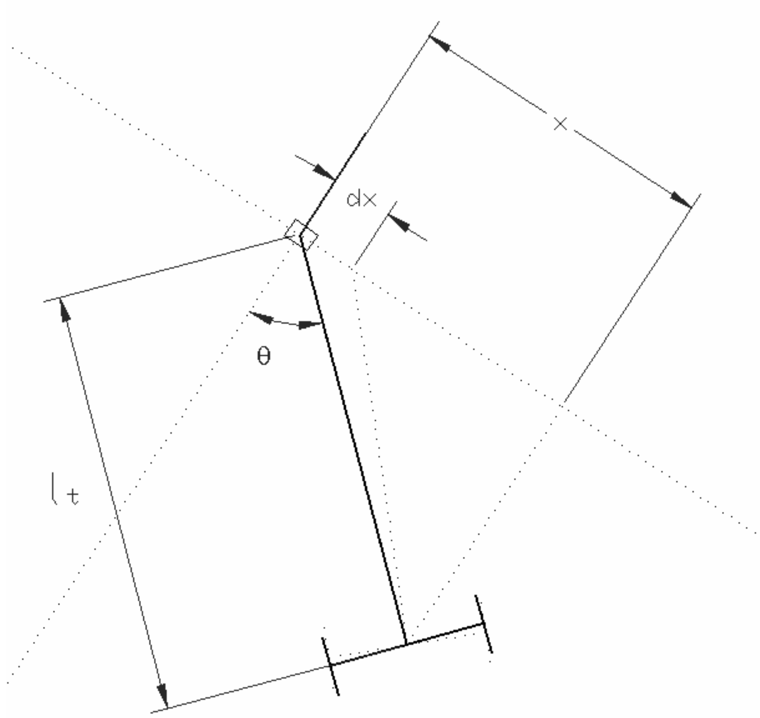

Figure 4-1: Imparted Slider Motion

The algorithm is illustrated in Figure 4-2.

Method II

A new variable ‘y’ is introduced that corresponds to the position of the center of the trailer axle, measured parallel to the slider. Ideally this point (y=0) would always be in line with the line through the center of axles of the vehicle. Thus the slider is moved to a position such that the trailer takes the angle just calculated. Now for some reason if the y value changes to some other value x is moved in such a way to position the trailer relative to the vehicle such that y equals zero again.

This method uses jackknifing to its own benefit. When the value of y isn't close to zero, the slider moves to a position such that the trailer begins to jackknife in the opposite direction and when y is at the desired value the slider moves back to its original position. This is illustrated in Figure 4-3.

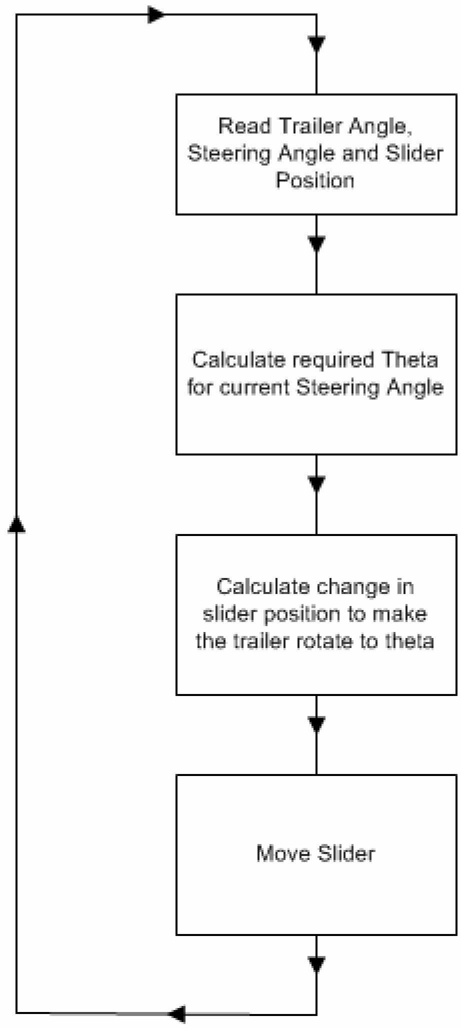

Figure 4-2: Algorithm for Method I

Besides this depending on the steering angle the initial value of x is calculated knowing the value of θ corresponding to every steering angle. Due to the lower processing power of the microprocessor the calculation of the desired trailer angles were done offline and some sample values are tabulated below. Interpolation is then used to calculate intermediate values. From this the x values were obtained.

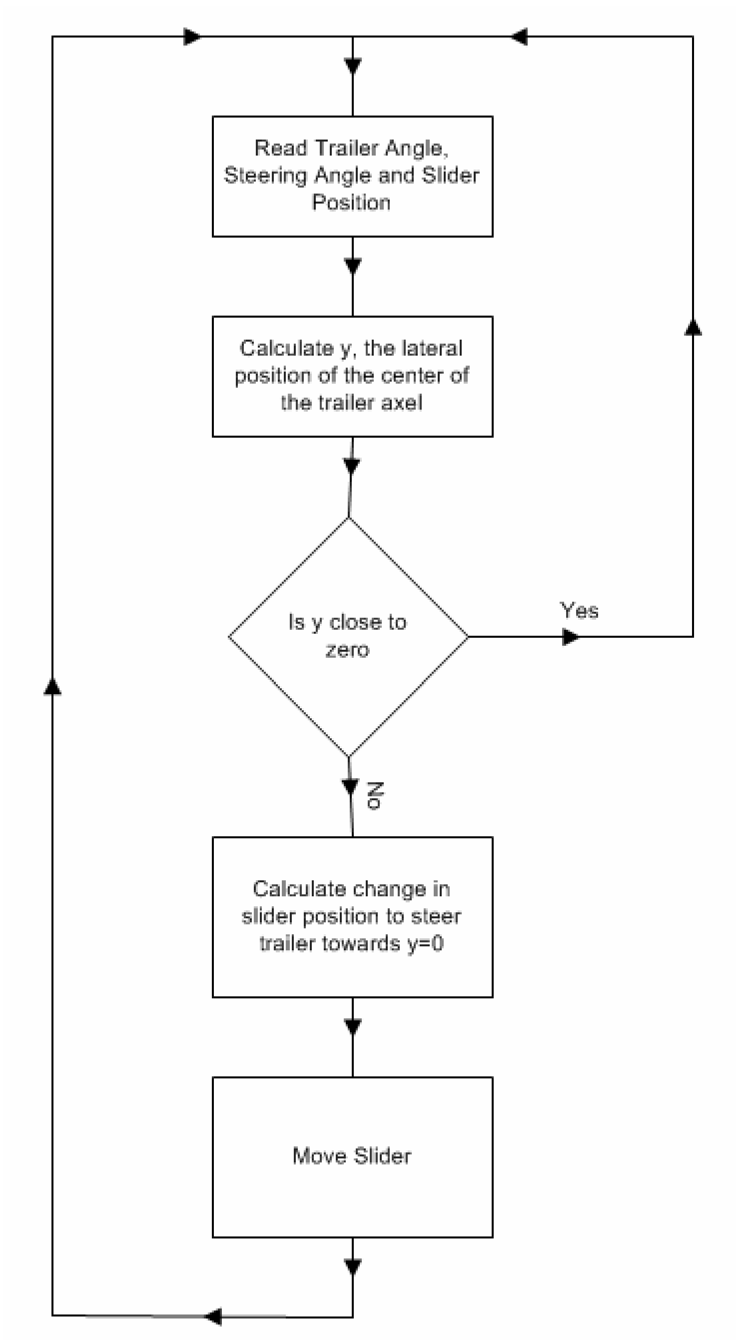

Figure 4-3: Algorithm for Method II

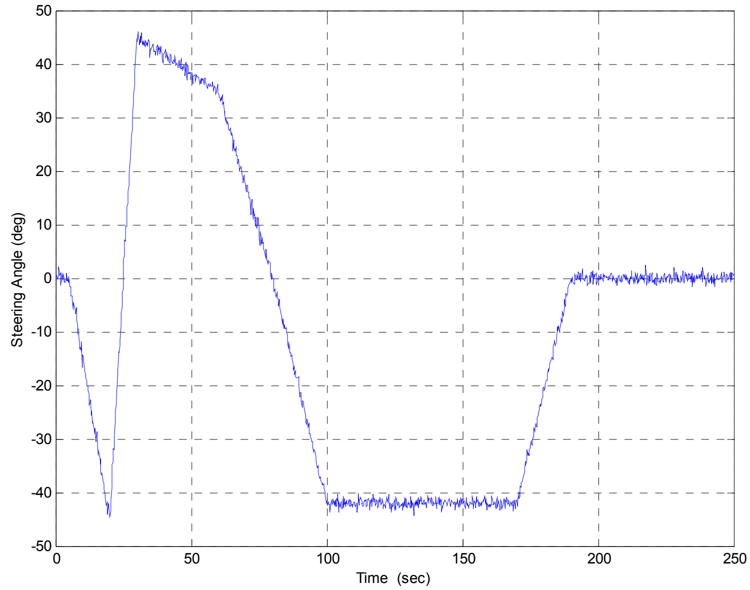

Figure A

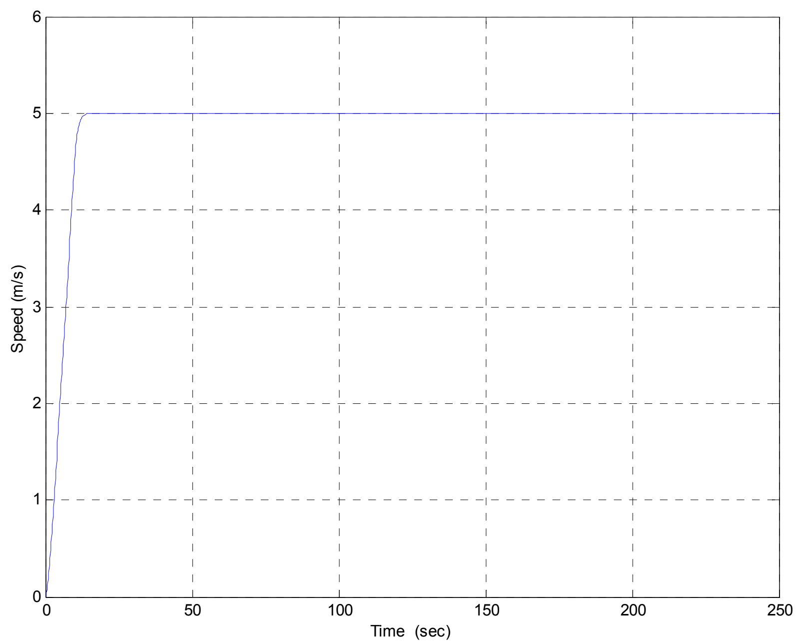

Figure B

Figure 4-4: Graphs of Input Parameters.

A) Steering Angle vs. Time B) Speed vs. Time

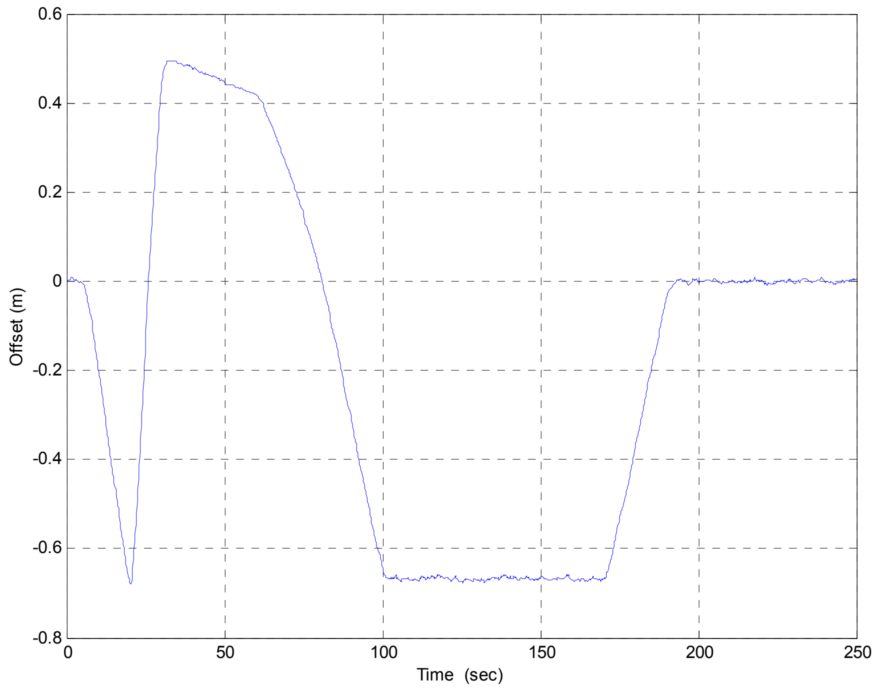

Figure 4-5: Offset vs. Time

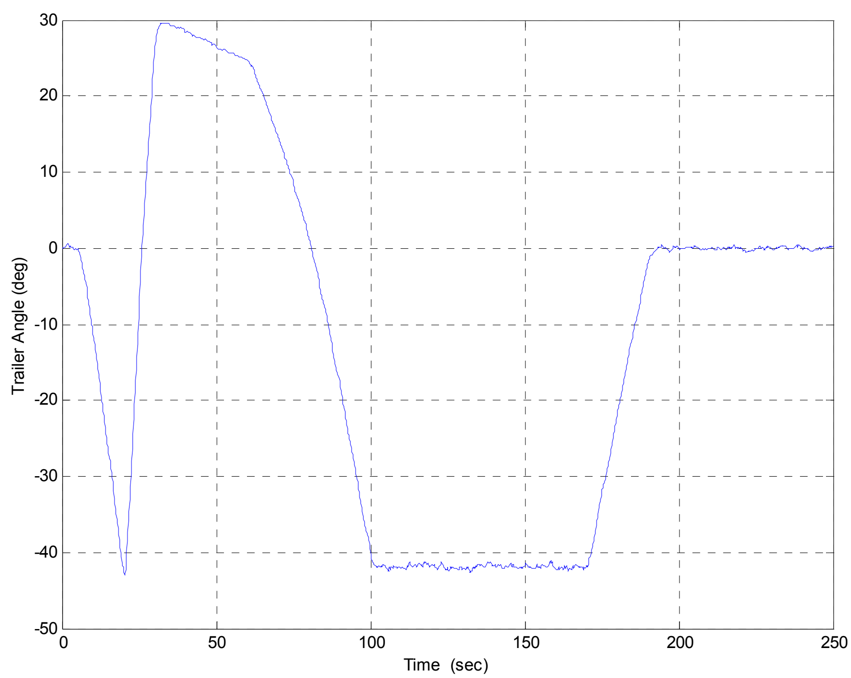

Figure 4-6: Trailer Angle vs. Time

ϕ	θ
-12	13.2649
-9	9.8876
-6	6.5631
-3	3.2730
0	0
3	-3.2730
6	-6.5631
9	-9.8876
12	-13.2649

Table 4-1: Sample Values for the Setup

Implementation

Simulink

The Simulink model involves recreating the system response of a vehicle-trailer model with introduction of the slider at the hinge of the trailer. This system implements the first algorithm described above. The second algorithm is implemented physically and hence isn't discussed here. The system takes the steering angle and the speed of the vehicle as input. Speed is taken as an input because the system response will vary depending on the speed of the vehicle because unlike the speed of the vehicle the slider can only move within limitations. Thus a vehicle backing up at a very high speed may not be easy to control. It also takes the current offset and the trailer angle as an input. From this it calculates the required offset and moves the slider to that position in order to compensate any change in the steering angle or change in trailer angle caused due to maybe uneven terrain. It also has noise in the steering angle input which helps recreate a more realistic model. The Simulink model is shown in the Appendix in more detail.

Below are the results of the simulation. The steering angle (Figure 4-4a) and the vehicle speed (Figure 4-4b) are the inputs to the system and accordingly the offset (Figure 4-5) is changed and thus the trailer's angle (Figure 4-6). Figure 4-7 shows the path that the vehicle follows and its orientation at various points on that curve.

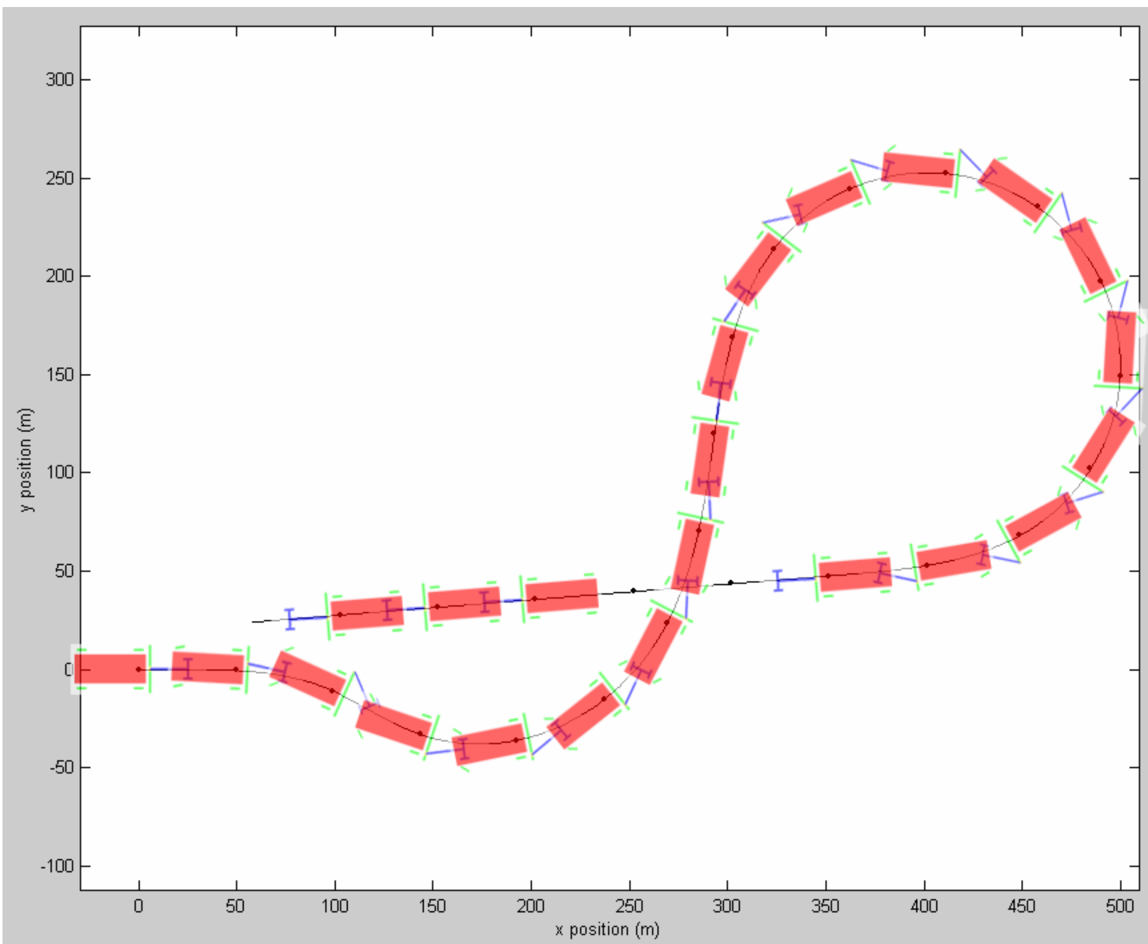

Figure 4-7: Path and Trailer Orientation

Physical Model

The physical model is built on a small remote controlled car. The vehicle features digital steering which allowed the steering angle of the car to be changed to any desired angle. The car was modified to attach a trailer and a slider.

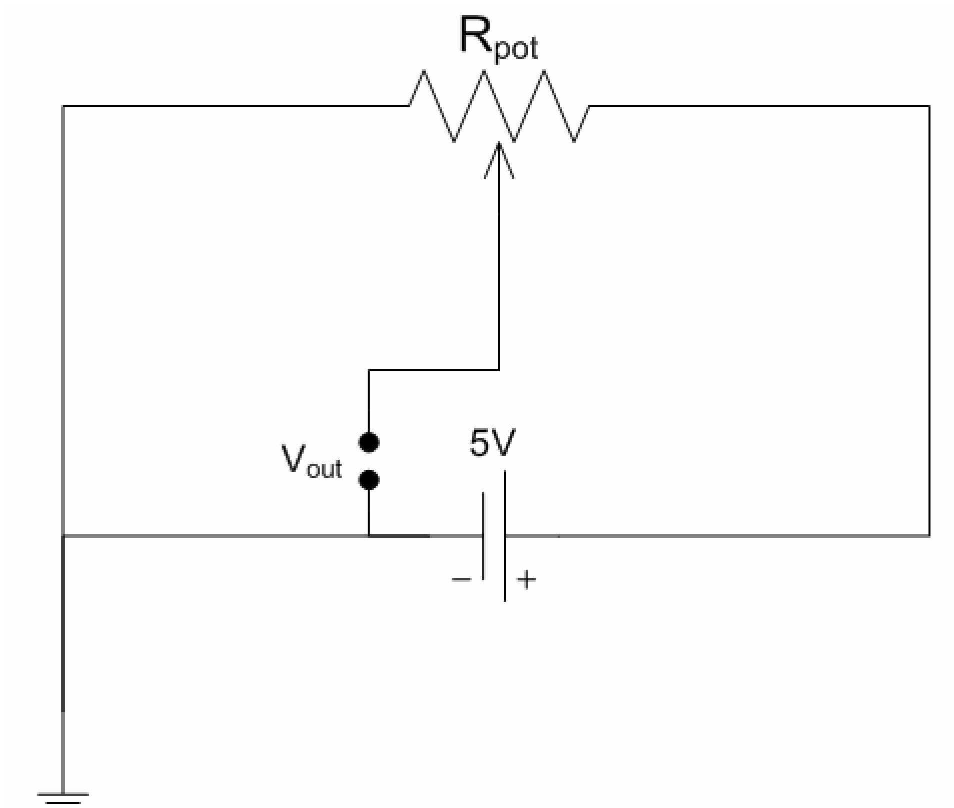

Figure 4-8: Traditional Resistor Setup

Data acquisition-Potentiometers

The potentiometers used were of the rotary type with outputs at the two ends and one on the wiper. The range of the potentiometer was approximately 180˚. This implied that the potentiometer's resistance between one of the end terminals and the wiper would change from almost zero to almost the resistance between the end terminals for a rotation of about 180˚ and vice versa for the other end terminal.

From the above setup (Figure 4-8) it is seen that the voltage can be varied across the resistor between 0 and 5 volts. However for the experimental setup a range of 45˚ to 135˚ is only required. Besides this in order to have a wider range of values it was also required to have the voltage at 45˚ relative to ground to be 0 and the voltage at 135˚ relative to ground to be 2.5.

In order to do this two unknown resistances R_1 and R_2 are added in series as shown in Figure 4-9.

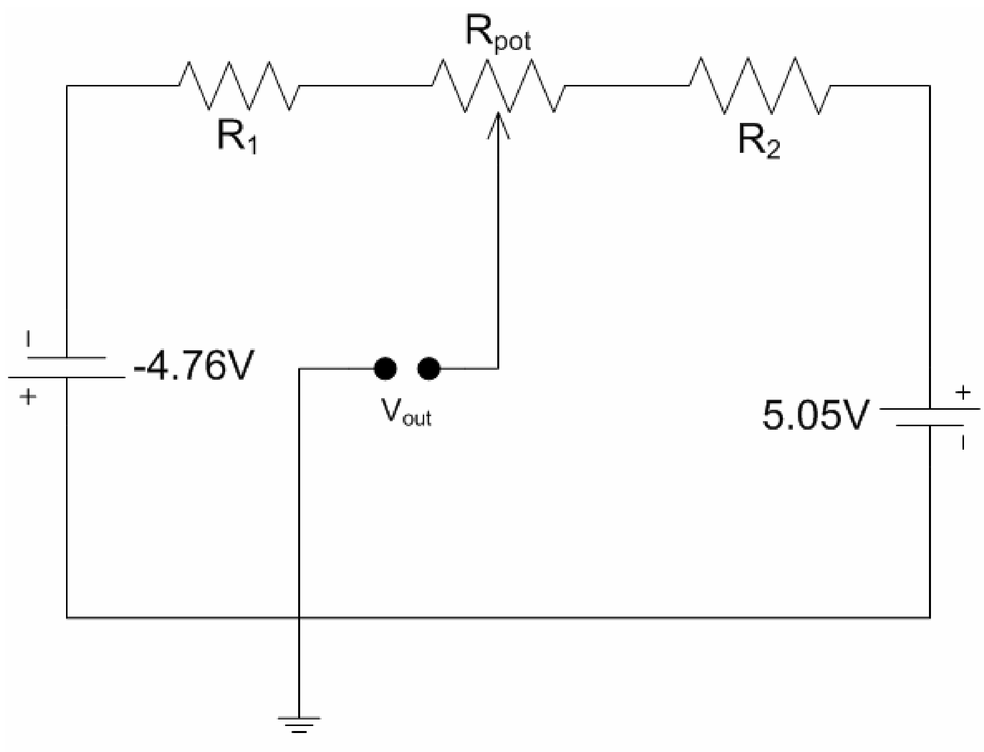

Figure 4-9: Modified Resistor Setup

$$R_{total} = R_1 + R_{pot} + R_2 \tag{4.2}$$

$$V_a = \frac{\left(R_1 + \frac{aR_{pot}}{180}\right)\left(V_h - V_l\right)}{R_{total}} + V_l \tag{4.3}$$

$$V_b = \frac{\left(R_1 + \frac{bR_{pot}}{180}\right)\left(V_h - V_l\right)}{R_{total}} + V_l \tag{4.4}$$

From these equations R_1 and R_2 is calculated as below

$$R_1 = -\frac{\left(-V_a b - aV_l + bV_l + V_b a\right)R_{pot}}{180\left(V_b - V_a\right)} \tag{4.5}$$

$$R_2 = -\frac{\left(aV_h - bV_h + V_a b - V_b a + 180V_b - 180V_a\right)R_{pot}}{180(V_b - V_a)} \tag{4.6}$$

Now in for this case the requirements were

$$\begin{aligned} R_{pot} &= 4.79k\Omega \\ a &= 45° \\ b &= 135° \\ V_l &= -4.76V \\ V_h &= 5.05V \\ V_a &= 0V \\ V_b &= 2.5V \end{aligned} \tag{4.7}$$

Thus

$$\begin{aligned} R_1 &= 3.276k\Omega \\ R_2 &= 1.245k\Omega \end{aligned} \tag{4.8}$$

Also in some cases the angle of the range may not be known but resistances at the end points are known. In that case let R_a and R_b be the resistances

$$V_a = \frac{\left(R_1 + R_a\right)\left(V_h - V_l\right)}{R_{total}} + V_l \tag{4.9}$$

$$V_b = \frac{(R_1 + R_b)(V_h - V_l)}{R_{total}} + V_l \tag{4.10}$$

From these equations R_1 and R_2 are calculated as below

$$R_1 = -\frac{(-V_b R_a + R_a V_l + V_a R_b - R_b V_l)}{(V_b - V_a)} \tag{4.11}$$

$$R_2 = -\frac{(R_a V_h - R_b V_h - V_b R_a + V_b R_{pot} + V_a R_b - V_a R_{pot})}{(V_b - V_a)} \tag{4.12}$$

Now in for this case the requirements were

$$\begin{aligned} R_{pot} &= 4.84k\Omega \\ R_a &= 2.075k\Omega \\ R_b &= 2.706k\Omega \\ V_l &= -4.76V \\ V_h &= 5.05V \\ V_a &= 0V \\ V_b &= 2.5V \end{aligned} \tag{4.13}$$

Thus

$$\begin{aligned} R_1 &= -0.896k\Omega \\ R_2 &= -1.490k\Omega \end{aligned} \tag{4.14}$$

Resistances can't be less than zero and so the range of the potentiometer was increased. R_a was decrease and R_b was increases by $500k\Omega$.

Thus

$$\begin{aligned} R_a &= 1.575k\Omega \\ R_b &= 3.206k\Omega \end{aligned} \tag{4.15}$$

This yielded

$$\begin{aligned} R_1 &= 1.471k\Omega \\ R_2 &= 0.029k\Omega \end{aligned} \tag{4.16}$$

The Servo

The servo is an actuation device that will rotate to any commanded position. The servo used takes three inputs. Two are for power out of which one is the common ground and the other is +5 volts. The third input is a PWM whose duty cycle controls the position of the servo to any desired angle within its range. The duty cycle of the PWM can be varied from between 10% to 20% with a time period of 20ms to get the servo to rotate between the zero position and the 180 degree position.

Dimensions (mm)	1.56 x 0.79 x 1.56 in. 39.5 x 20.0 x 39.6 mm
Weight	46 Grams / 1.62 oz
Ball Bearings	Yes, 2BB
Metal Gears	No
Torque (4.8V)	69 oz.in.
Transit Time (4.8V)	0.21 sec./60°
Torque (6.0V)	86 oz.in.
Transit Time (6.0V)	0.17 sec./60°

Table 4-2: High-torque Ball-bearing Servo Motor from GWS

The Prototype

Rotary to Linear Conversion

The rotary motion of the servo is converted to a linear motion by means of a pulley – slider system. The setup is shown in Figure 4-11 and 4-12.

When the pulley rotates the slider moves changing the trailer angle as it does this. In Figure 4-13 the slider is moved to the left forcing the trailer to change its angle.

Figure 4-13 shows the linking of the pulley with the slider along the back of the vehicle. Figure 4-14 shows the mounting of the pulley on the servo attached to the body of the vehicle.

Figure 4-10: High-Torque Ball-Bearing Servo Motor from GWS

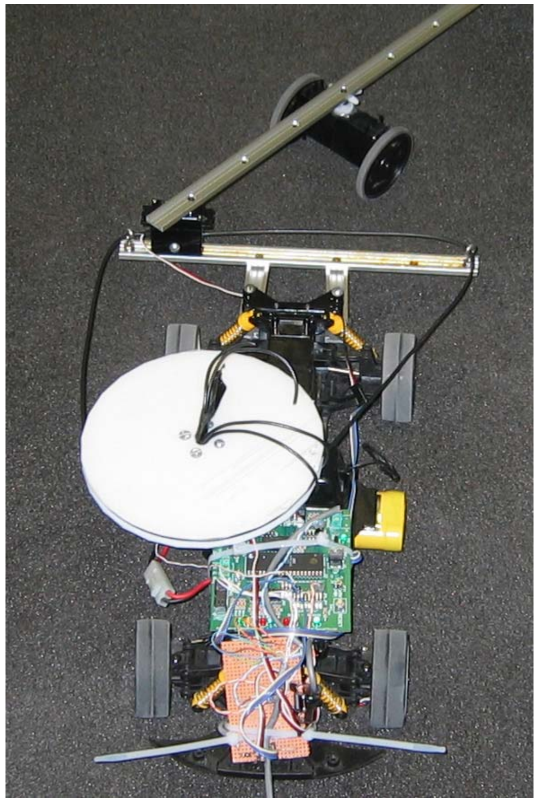

Figure 4-11: The Prototype Setup – I

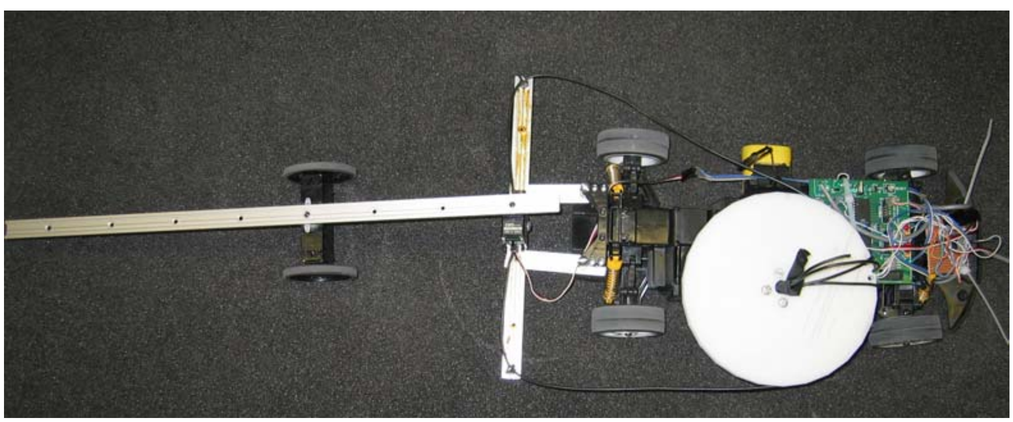

Figure 4-12: The Prototype Setup – II

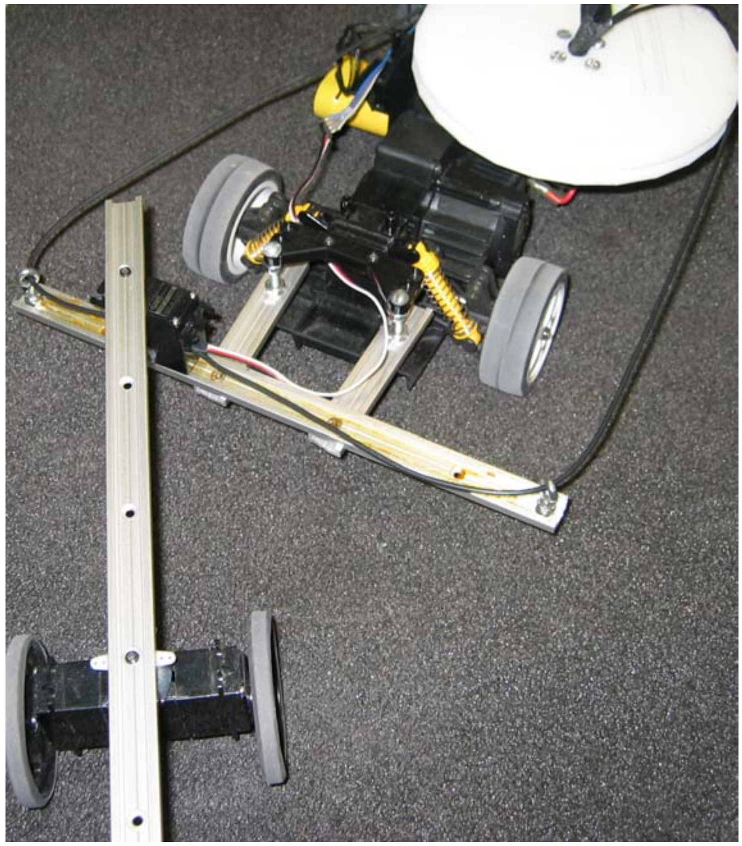

Figure 4-13: The Working of the Slider

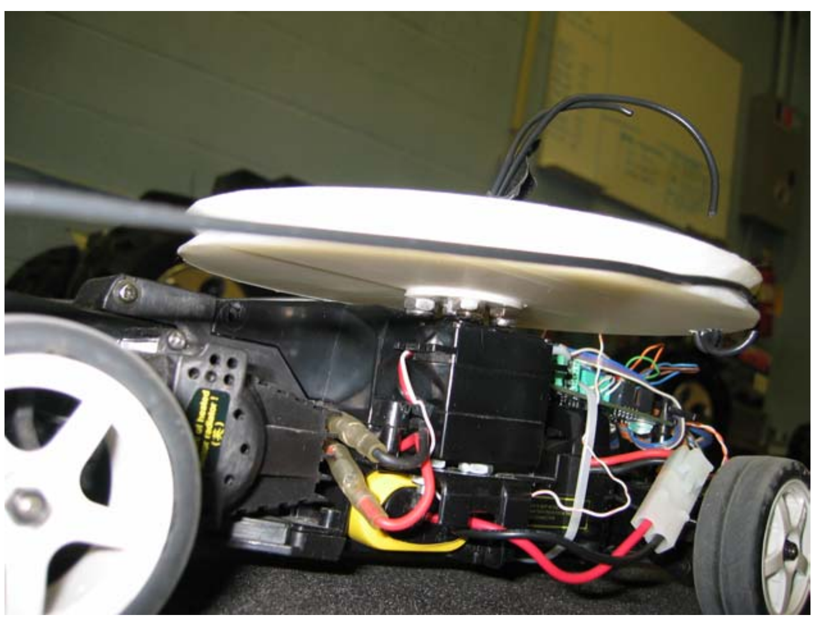

Figure 4-14: Mounting of the Pulley on the Servo

Mounting of Potentiometers

Trailer angle potentiometer

The potentiometer to read the trailer angle is mounted inside a servo casing and attached to the slider. This is seen in Figure 4-15.

Steering angle potentiometer

The potentiometer to read the steering angle is mounted below the hinge for one of the front wheels of the car. Although this gives the reading for only one wheel and not the average, it was found that this value was sufficient to get the prototype to work. The mounting is shown in Figure 4-16.

x value feedback potentiometer

The servo though very accurate in getting to a position that is requested like any mechanical system takes a while to get where it is commanded. However the servo used did not have any feedback to let the microcontroller know what its current position was. Thus a modification had to be made so that is would output its current position. This was done by tapping the potentiometer built into the servo and calculating the voltage drop across it.

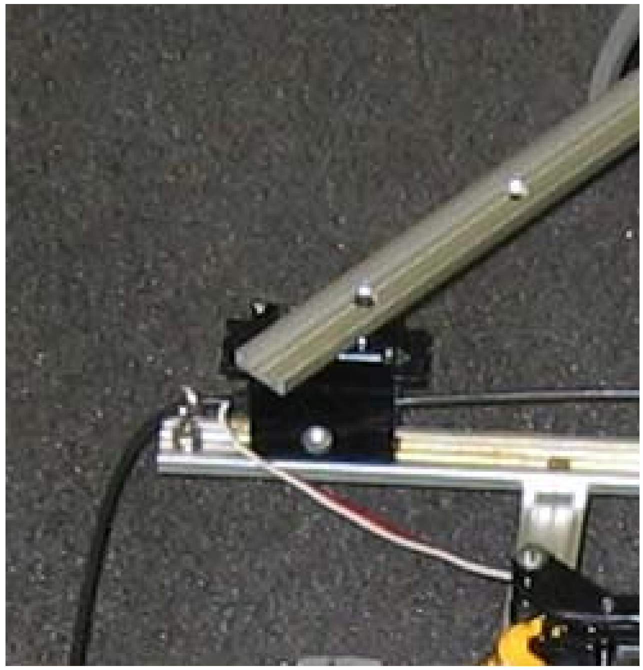

Figure 4-15: Trailer Angle Potentiometer

Of course the best way to get the value of X would be to actually introduce a linear transducer on the slider. However, this wasn't cost effective and would make the slider very large and also be an additional load on the servo, decreasing its response time. Reading the position off the servo gave the value of x within a reasonable level of accuracy and so this value was converted and used.

Approximation of Sine Using Taylor Series Expansion

Given a function whose first n derivatives can be found, the Taylor polynomial $P_n(x)$ of degree n for the function $f(x)$ is defined about the value c as [19]

$$P_n(x) = f(c) + f'(c)(x-c) + \frac{f''(c)(x-c)^2}{2!} + \frac{f'''(c)(x-c)^3}{3!} + \ldots + \frac{f^{(n)}(c)(x-c)^n}{n!} \quad \ldots (4.17)$$

where $f^{(n)}(c)$ denotes the n$^{\text{th}}$ derivative of the function f evaluated at $x = c$.

It is required to find the Taylor Series expansion for

$$f(x) = \sin x \tag{4.18}$$

The derivatives of $\sin x$ are first found and then evaluated at $c = 0$ (A Taylor Series at $c = 0$ is also known as a MacLaurin series)

n	$f^{(n)}(x)$	$f^{(n)}(c)$
0	$\sin x$	0
1	$\cos x$	1
2	$-\sin x$	0
3	$-\cos x$	-1
4	$\sin x$	0
5	$\cos x$	1
6	$-\sin x$	0
7	$-\cos x$	-1
8	$\sin x$	0
9	$\cos x$	1
10	$-\sin x$	0

Table 4-3: Taylor Substitution

$$\sin x = f(c) + f'(c)(x-c) + \frac{f''(c)(x-c)^2}{2!} + \frac{f'''(c)(x-c)^3}{3!} + \ldots + \frac{f^{(n)}(c)(x-c)^n}{n!} \ldots \tag{4.19}$$

$$\sin x = \sin(0) + \cos(0)(x-0) + \frac{-\sin(0)(x-0)^2}{2!} + \frac{-\cos(0)(x-0)^3}{3!} + \ldots \tag{4.20}$$

$$\sin x = x - \frac{x^3}{3!} + \frac{x^5}{5!} - \frac{x^7}{7!} + \frac{x^9}{9!} \ldots \tag{4.21}$$

Similarly for

$$f(x) = \cos x \tag{4.22}$$

$$\cos x = 1 - \frac{x^2}{2!} + \frac{x^4}{4!} - \frac{x^6}{6!} + \frac{x^8}{8!} + \ldots \tag{4.23}$$

The assumption of $\sin(x) = x$ for small values of x can be verified by truncating the Taylor Series to just the first order term. The results are seen in the plot Figure 4-17.

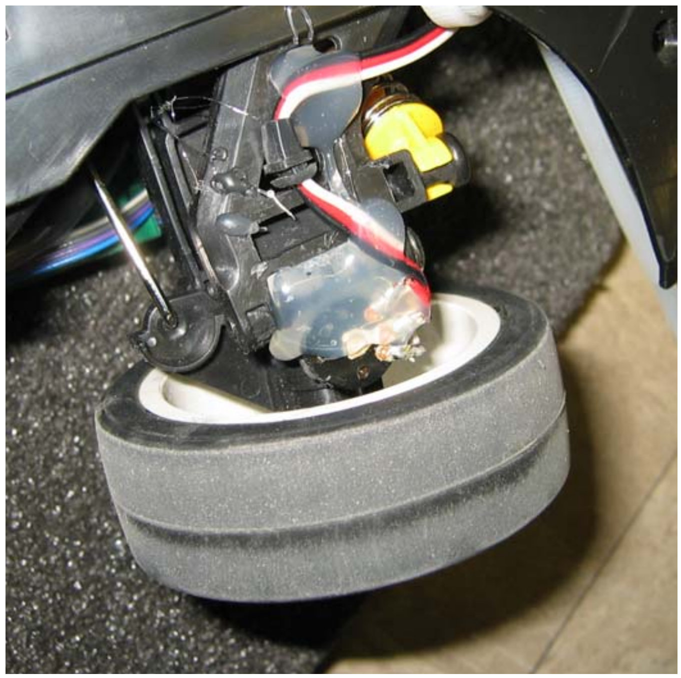

Figure 4-16: Steering Angle Potentiometer

Since the processor used wasn't very powerful a check was done to see how long an approximation of the Taylor series was required to get sufficiently accurate values for sine and cosine. Below are plots for truncated series of sine and cosine based on the order of the assumption. Figure 4-17, 4-18, 4-19, and 4-20 show the sine value approximated in red to the first order, third order, fifth order and seventh order respectively. The actual sine plot is also there in blue to show a comparison. Figure 4-21 shows the error between the actual value and the value obtained for all the series truncations. A strange feature is noticed with the 5th order approximation of sine which appears to be more accurate than the 7th order approximation.

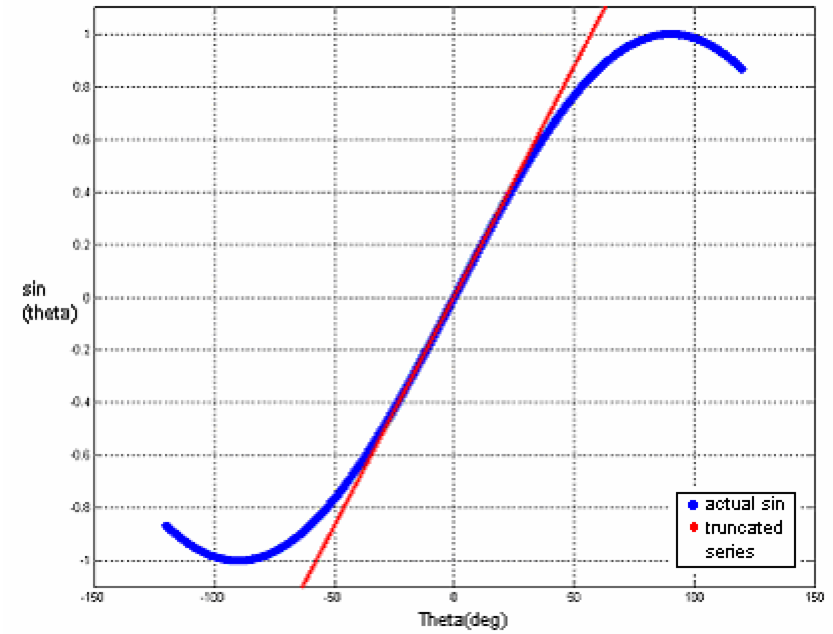

Figure 4-17: 1st Order Series Truncation - $\sin x = x$

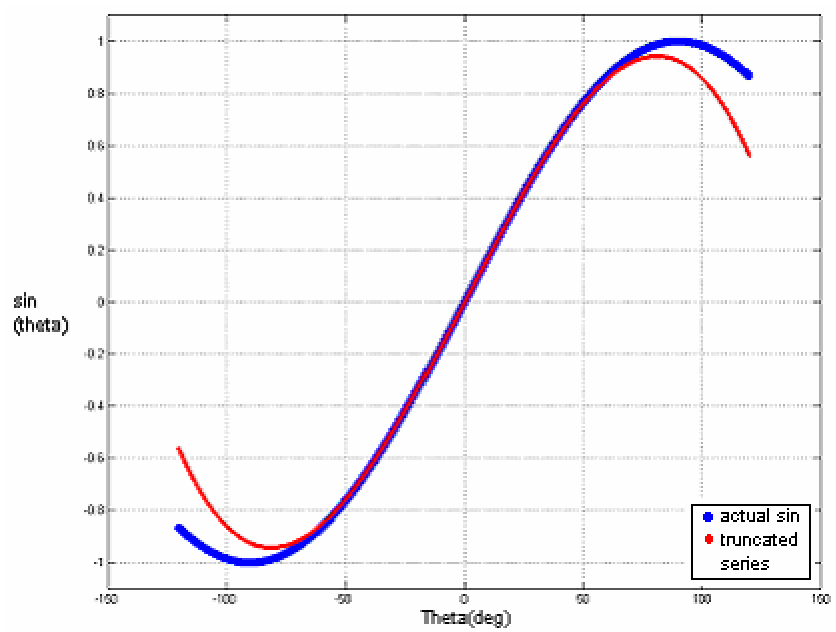

Figure 4-18: 3rd Order Series Truncation - $\sin x = x - \frac{x^3}{3!}$

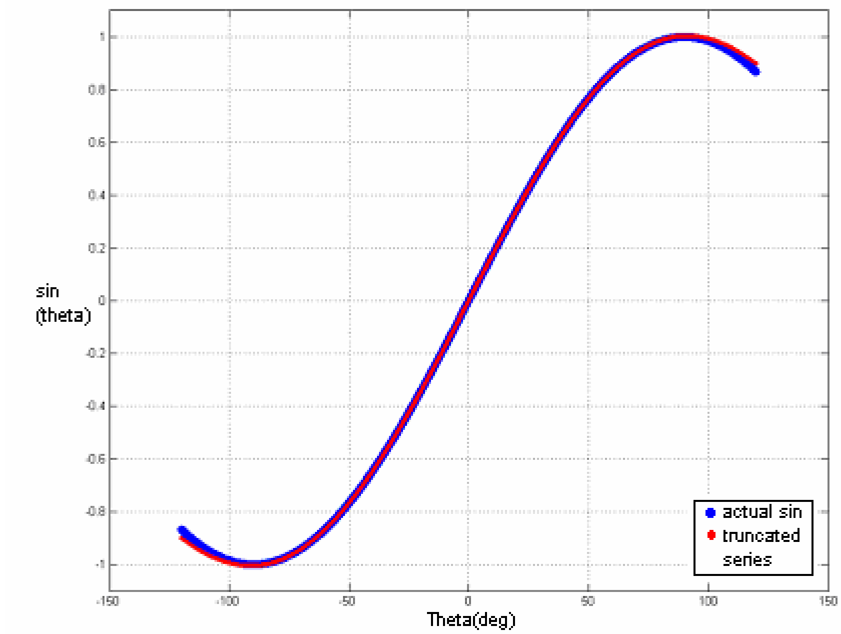

Figure 4-19: 5th Order Series Truncation - $\sin x = x - \frac{x^3}{3!} + \frac{x^5}{5!}$

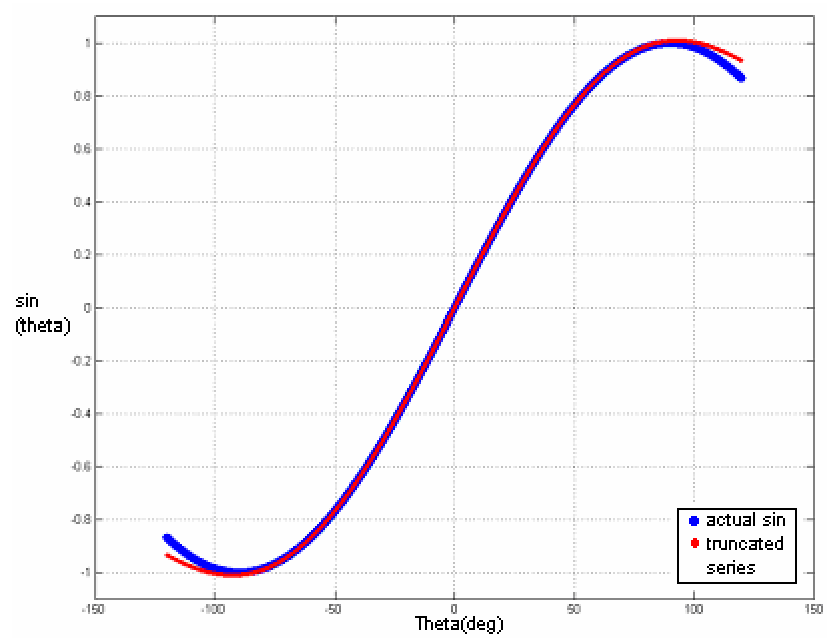

Figure 4-20: 7th Order Series Truncation - $\sin x = x - \frac{x^3}{3!} + \frac{x^5}{5!} - \frac{x^7}{7!}$

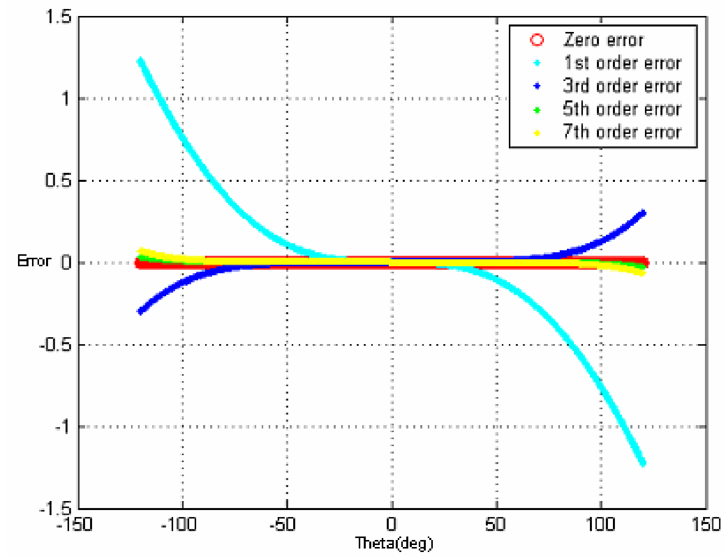

Figure 4-21: Error Plots for Sine Approximation

It is seen from the above graphs that the 5th order sine gives sufficient accuracy in the range of -90˚ to 90˚. Thus

$$\sin x == x - \frac{x^3}{3!} + \frac{x^5}{5!} \tag{4.24}$$

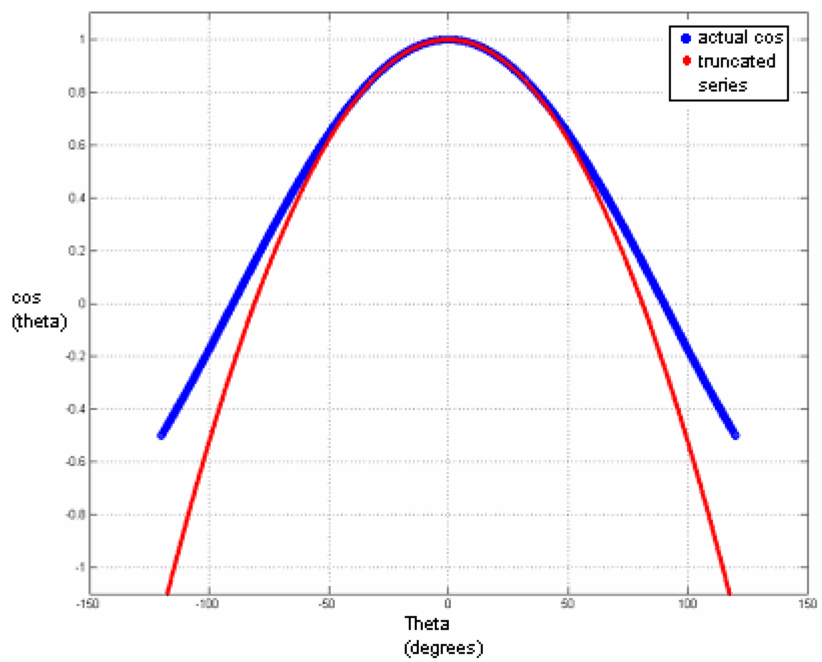

Figure 4-22: 2nd Order Series Truncation - $\cos x = 1 - \frac{x^2}{2!}$

A similar analysis is done for the cosine plots in Figures 4-22 to 4-25.

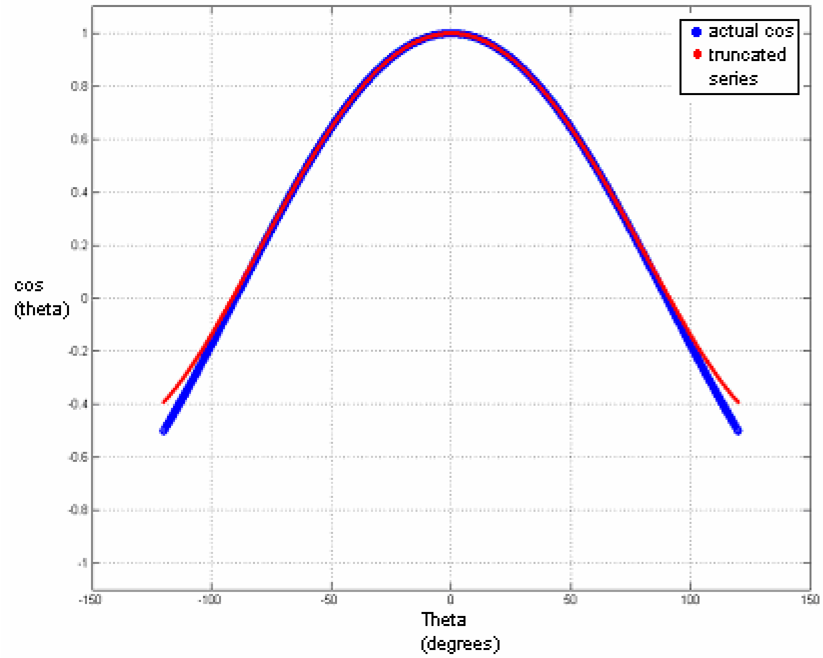

Figure 4-23: 4th Order Series Truncation - $\cos x = 1 - \frac{x^2}{2!} + \frac{x^4}{4!}$

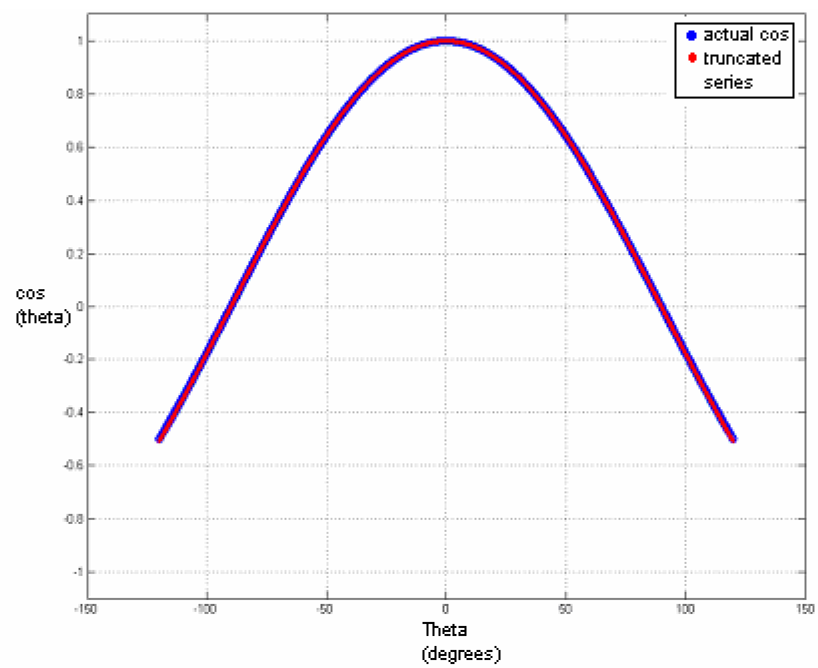

Figure 4-24: 6th Order Series Truncation - $\cos x = 1 - \frac{x^2}{2!} + \frac{x^4}{4!} - \frac{x^6}{6!}$

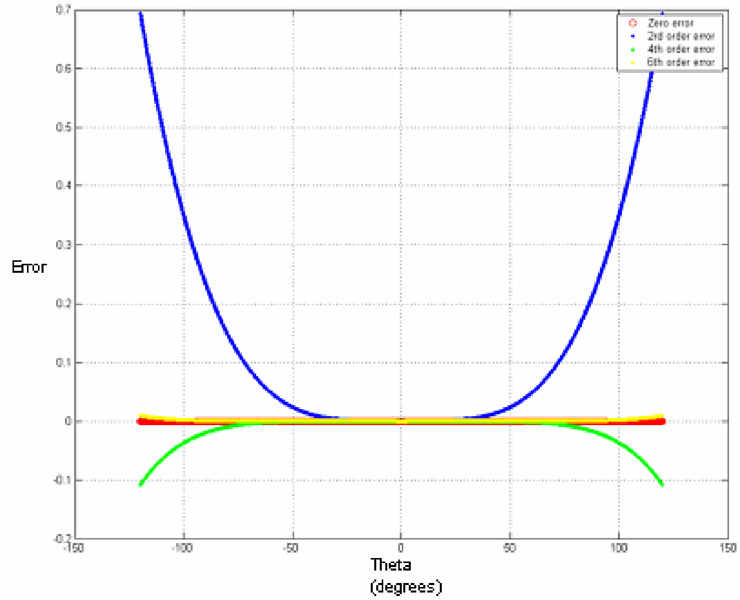

Figure 4-25: Error Plots for Cosine Approximation

It is seen from the above graphs that the 6th order cosine gives sufficient accuracy in the range of -90˚ to 90˚. Thus

$$\cos x = 1 - \frac{x^2}{2!} + \frac{x^4}{4!} - \frac{x^6}{6!} \tag{4.25}$$

Implementation

The model was build and programmed as per the second algorithm described above. The results of the tests run on the model are described in the next chapter.

CHAPTER 5
RESULTS AND CONCLUSIONS

A control loop was written to change the position of the slider based on the second method of implementation as described in the previous chapter.

To best illustrate the working of the algorithm the vehicle was backed up and the data was acquired into a computer and plotted. The values read in were the current values of steering angle, x (slider position) and trailer angle. Pictures were also taken at some positions to illustrate the data. y is calculated for each point and plotted too. For ease of understanding the time scale is divided in sections labeled A-L.

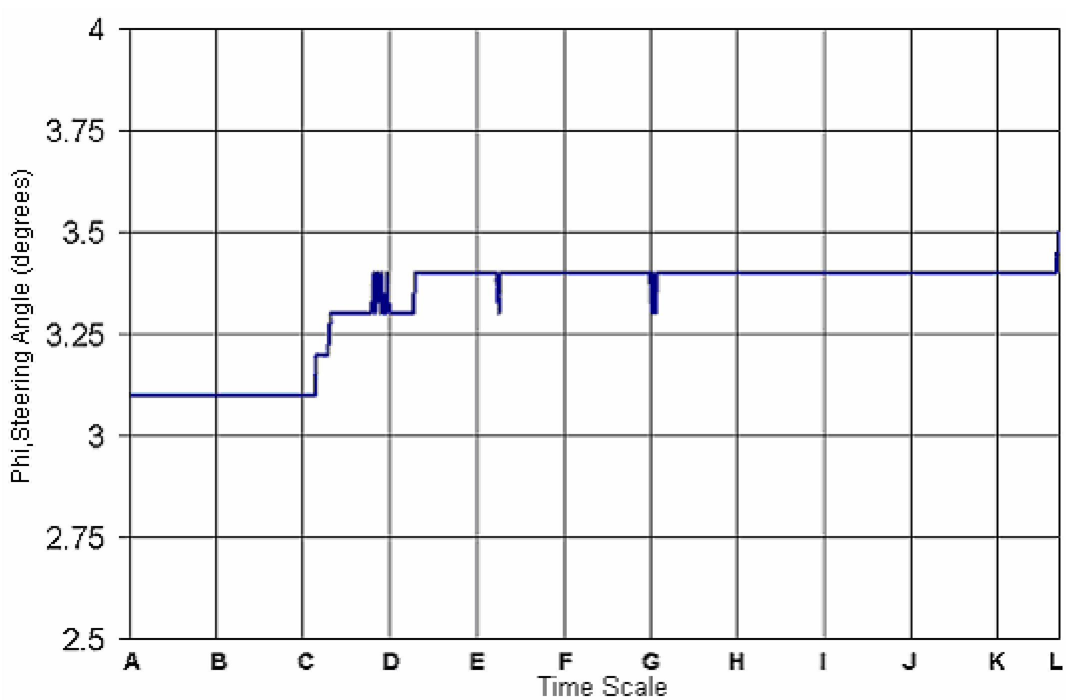

Figure 5-1: Steering Angle Acquired at Each Time Step

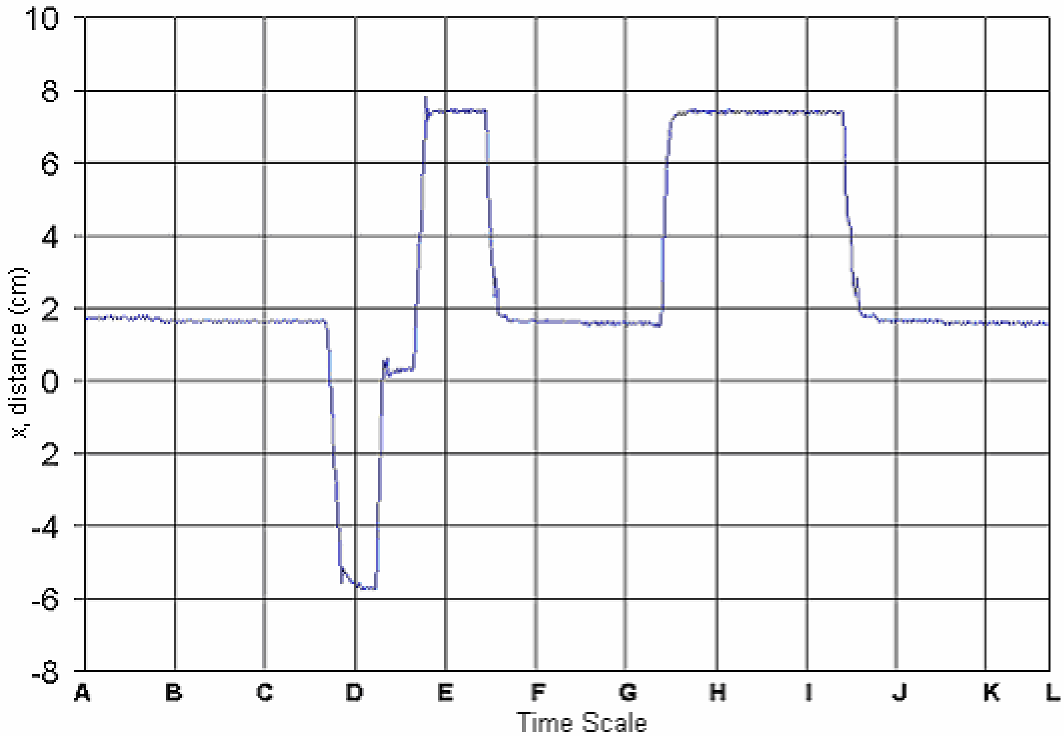

Figure 5-2: Slider Displacement, x, at Each Time Step

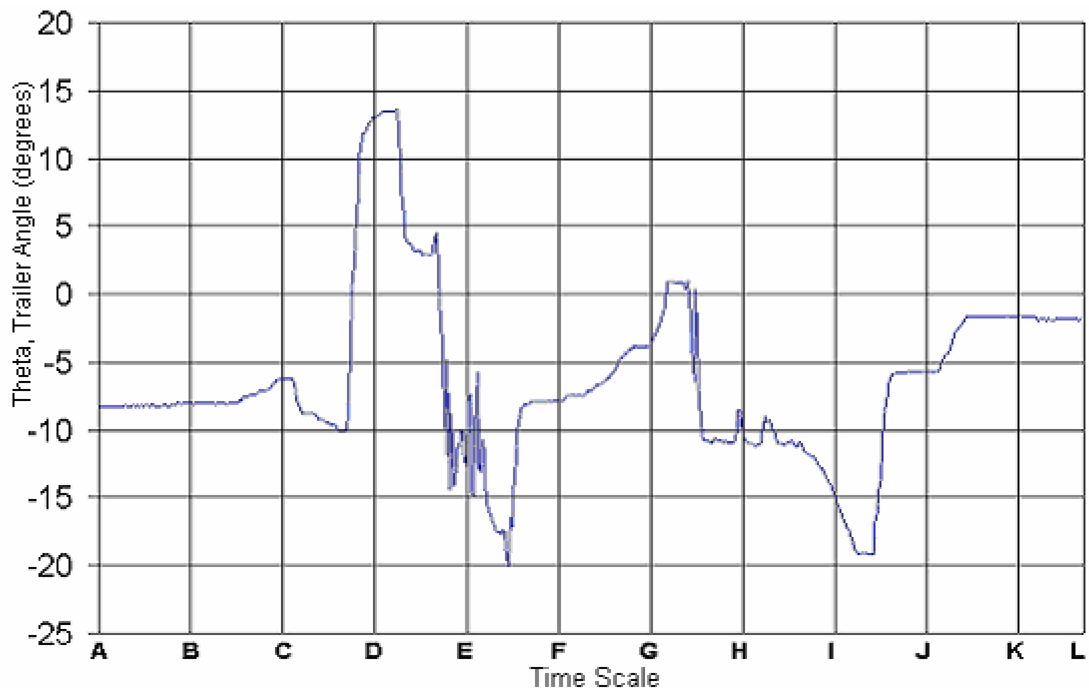

Figure 5-3: Relative Angle θ at Each Time Step

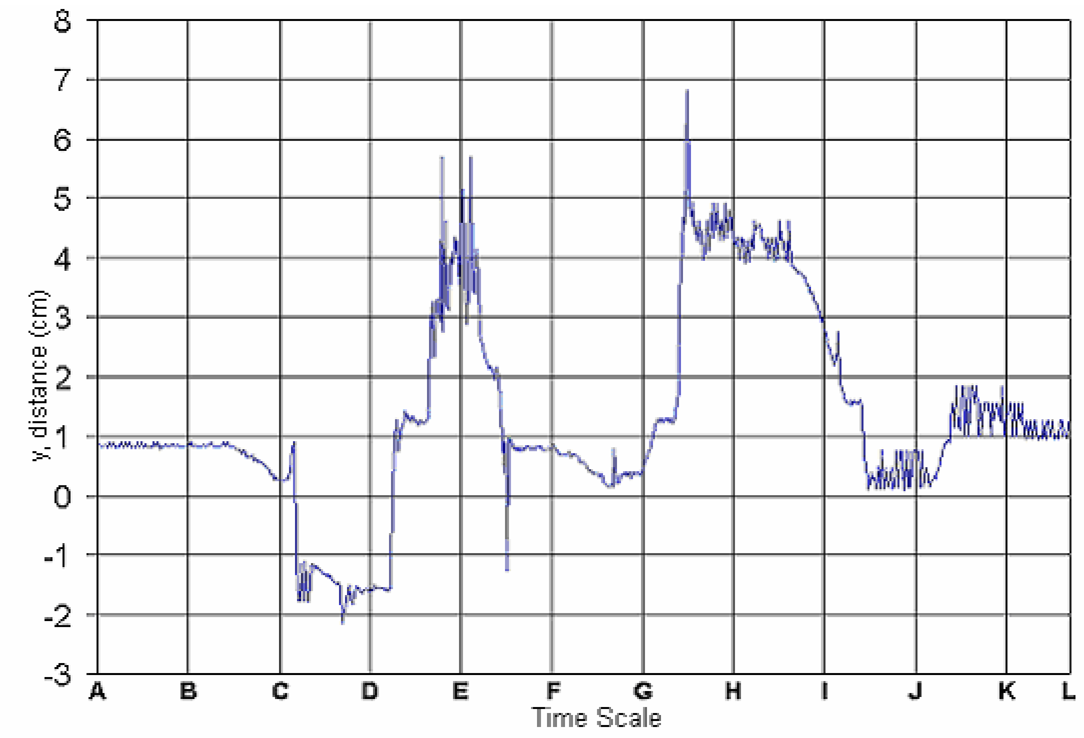

Figure 5-4: Value of y(cm) at Each Time Step

From Figure 5-1 it is seen that the steering angle remains practically stable at about 3˚. The change that occurred is due to the flexibility in the steering system. The vehicle is considered to be stable when the value of y lies between -1.5 to 1.5 cm. The stable condition is defined as the state at which the trailer is least likely to jackknife. For a steering angle of 3 degrees the appropriate required trailer angle is about -3.3°.

Until time step C the vehicle isn't moving. The trailer angle till this point remains stable at about -8°.

As the vehicle backs up the trailer angle decreases to beyond -10°, thus increasing the value of y to below -1.5 cm. Thus the slider changes the value of x to around -6cm between C and D.

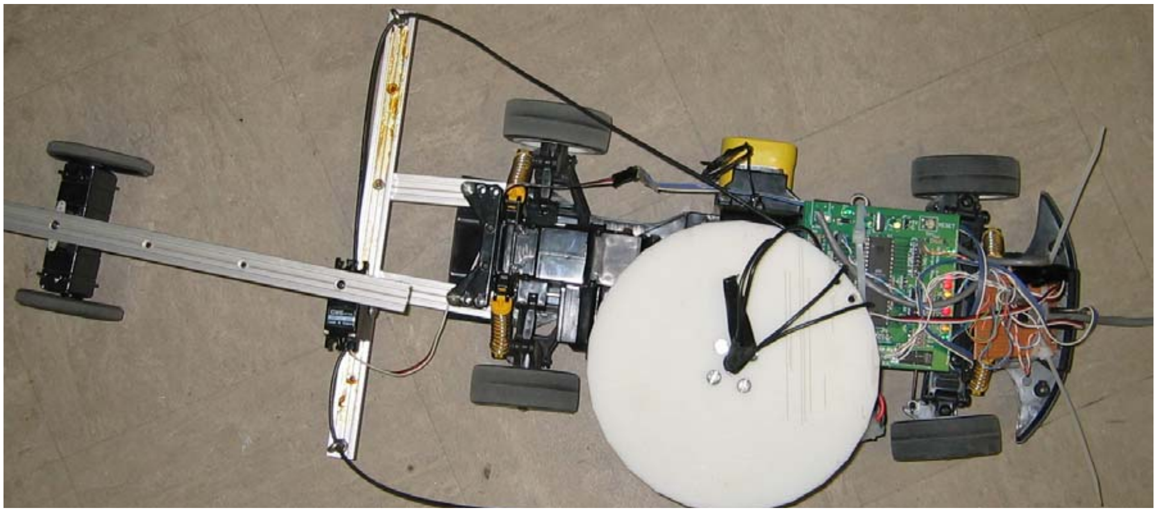

Figure 5-5: At A and B

Figure 5-6: At D

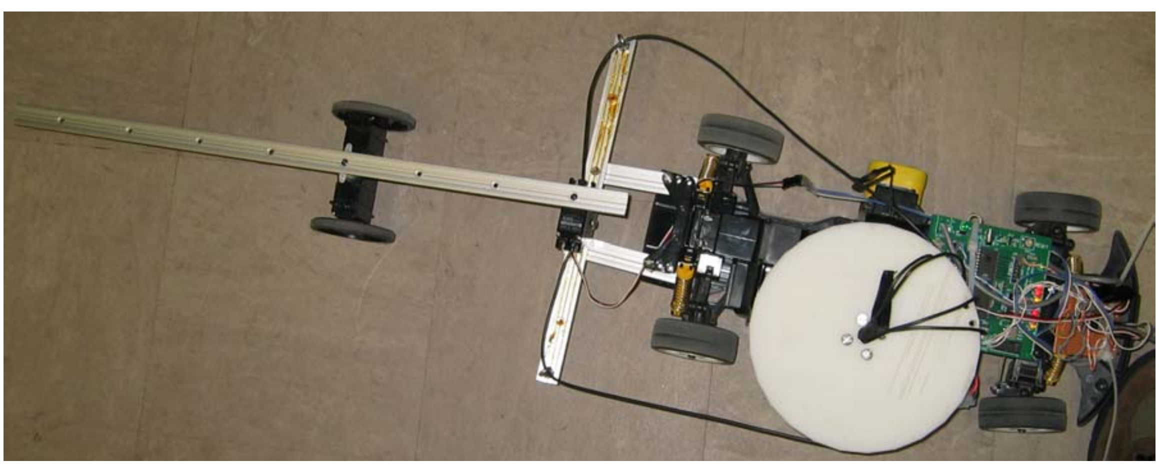

Figure 5-7: Between D and E

This changes θ to about 13° and as the vehicle backs up y begins to change until it reaches a position that is within the tolerable limits. At this point, between D and E the slider returns to its normal position.

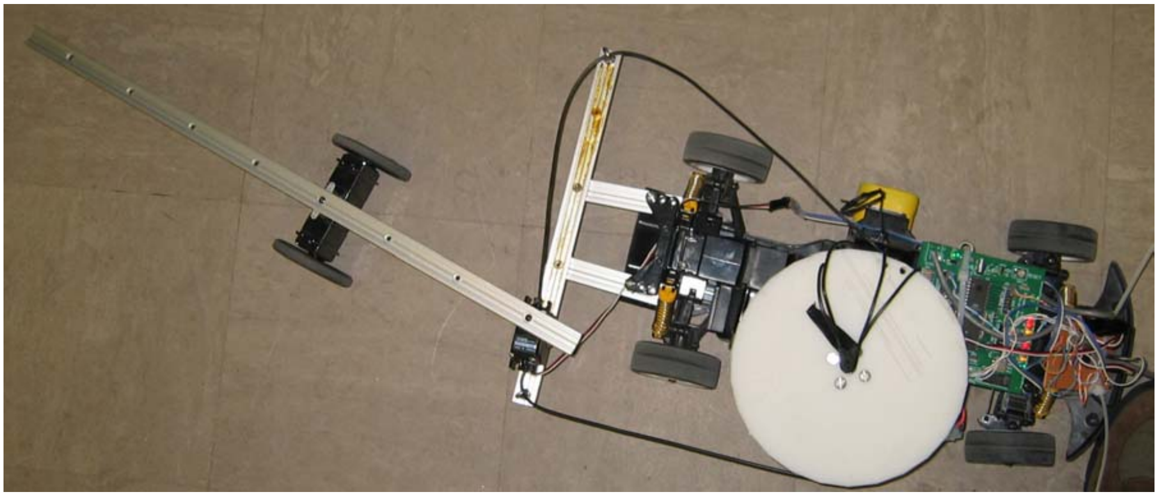

Figure 5-8: At E

However the slider does not react very fast. As a result the θ value again goes out of sync and begins to reduce. To compensate the slider now moves to +8.5cm between E and F, remaining at that position till the value of y reaches within the allowable range.

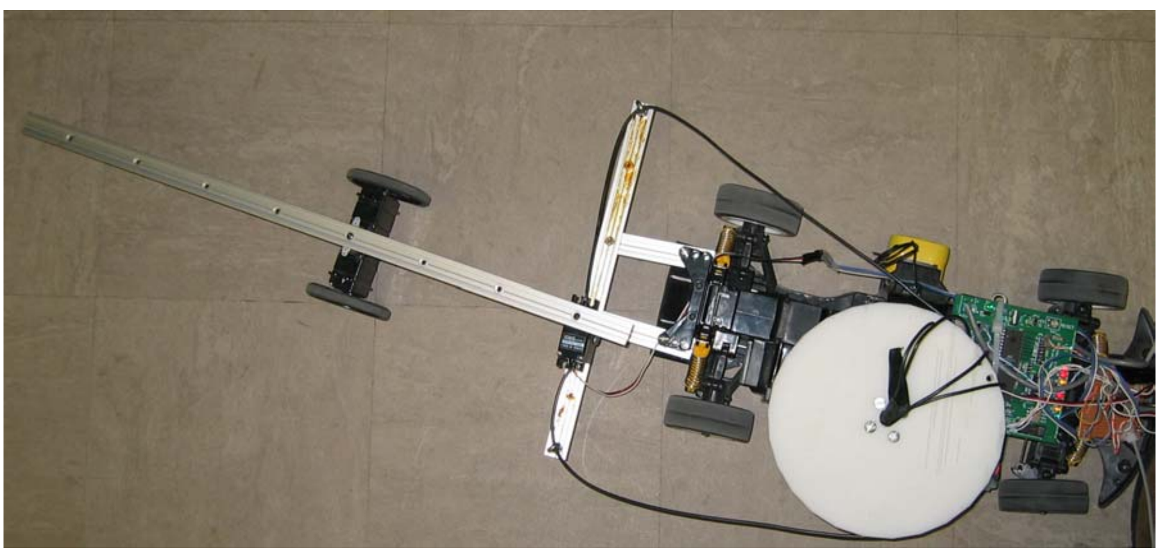

Figure 5-9: Between F and G

Figure 5-10: Between G and H

Figure 5-11: At H and I

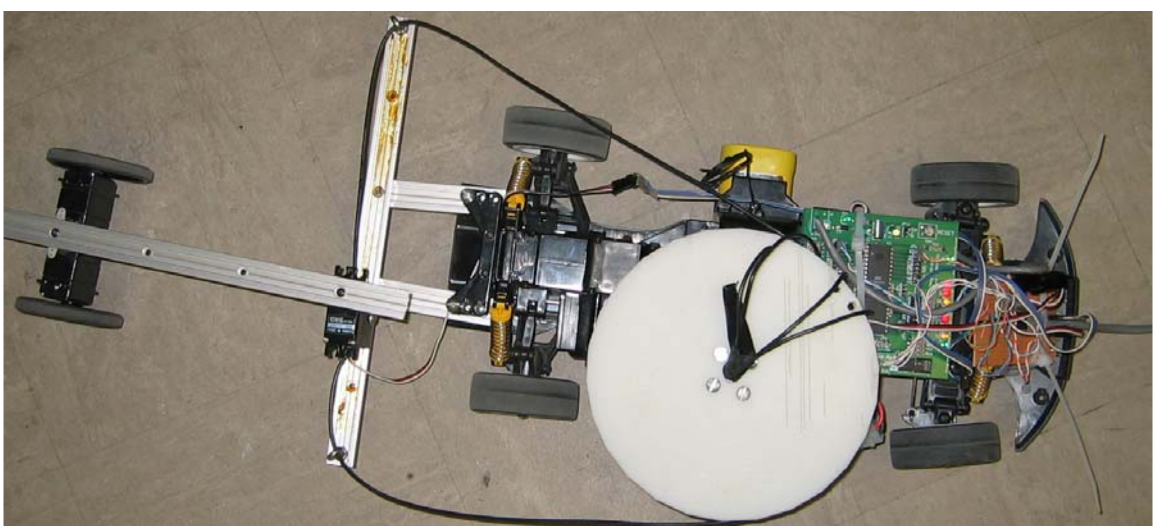

Figure 5-12: At J, K and L

The slider then moves back to the normal position and over a period of time the trailer regains its correct θ at about G. Similar corrections occur until time step J and the system thereafter remains stable.

Thus it is seen the system remains stable so that backing up doesn't cause the trailer to jackknife. The trailer is able to back up with reasonable efficiency at a reasonable speed.

An added benefit discovered was that while the vehicle is moving forward and negotiating a turn the slider can move outward causing the trailer to make a wider turn. This means that the vehicle will not have to make wide turns when turning sharp. Thus when a trailer is attached to the vehicle the vehicle can now drive forward also to an extent without worrying about the trailer.

The mechanism discussed in this thesis is simple enough to implement on almost any vehicle, be it autonomous or regular. The addition enables any driver without any particular skills in trailer backing to be able to back a vehicle up through any path.

As far as future work goes, methods can be introduced to increase the efficiency of the backing system so that the slider doesn't have to travel as much as it currently does. This would enable the trailer to move more efficiently and follow the vehicle's path more closely. Also, as on now the vehicle is the one that is being modified. Work can be done such that the attachment is made on the trailer and so it can be used on any vehicle by the simple attachment of a steering sensor.

APPENDIX
SOFTWARE MODEL OF THE TRAILER PROBLEM

The following is the software model of the vehicle-trailer system. The basic blocks shown in Figure A-1 are the system process block which outputs to an animation block. The system process block takes its input from the constants definition block and also a predefined steering angle and velocity values described later. Theta is the angle of the trailer, the offset is the distance of the slider from its central position and ‘a’ is the turning radius of the vehicle.

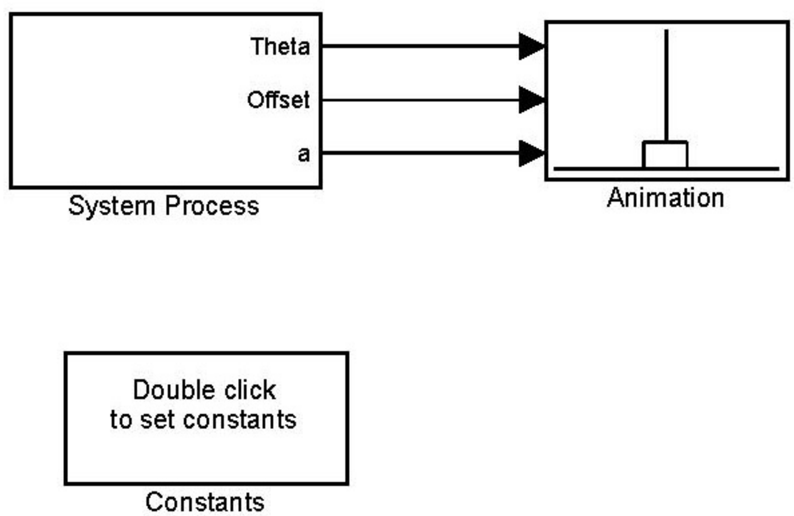

Figure A-1: Base Model

Figure A-2, A-3 and A-4 are the constant setting blocks. The vehicle width, distance of trailer hitch (off-hooking), length of trailer and distance of rear and front axels (wheel base) can be set here so that they are accessible by the model at any time.

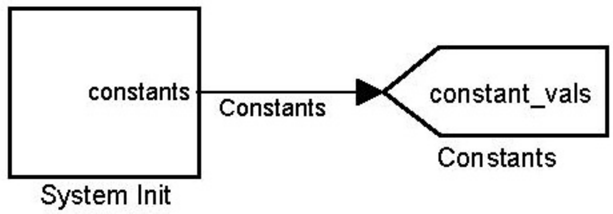

Figure A-2: Setting System Constants – Masked

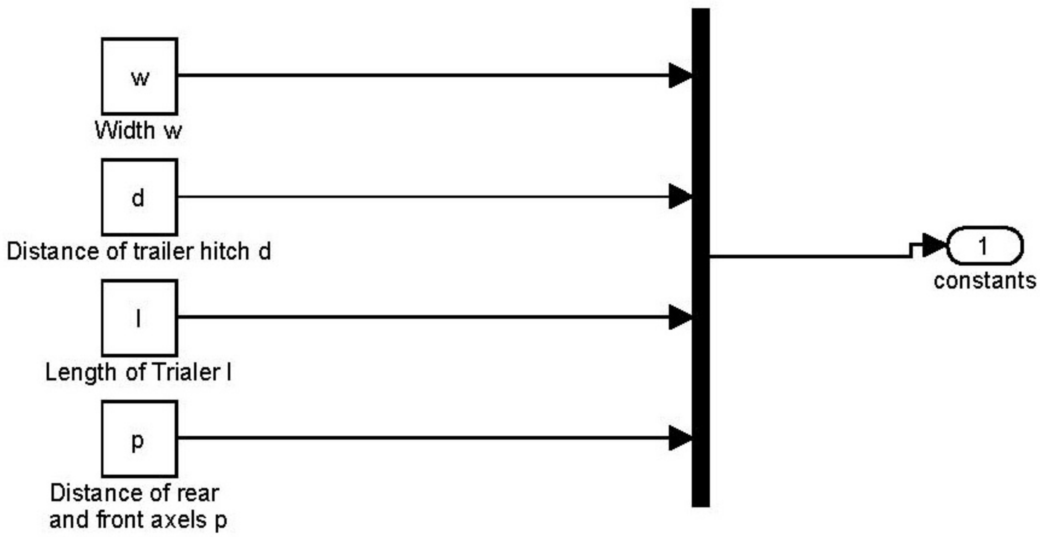

Figure A-3: Setting System Constants – Under the Mask

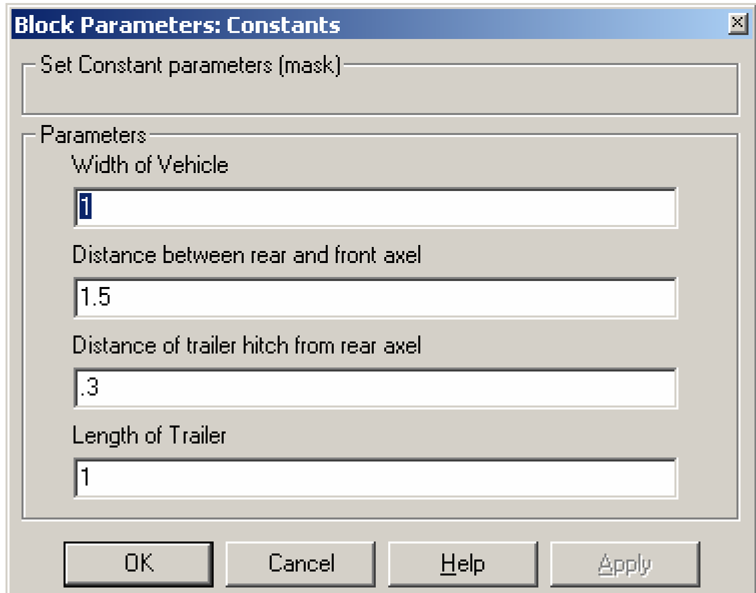

Figure A-4: Setting System Constants – Dialog Box

Figures A-5, A-6 and A-7 show how the vehicle speed is read from a data file and sent to the system. There is a delay block and a saturation block to make the system response to velocity commands slower in response.

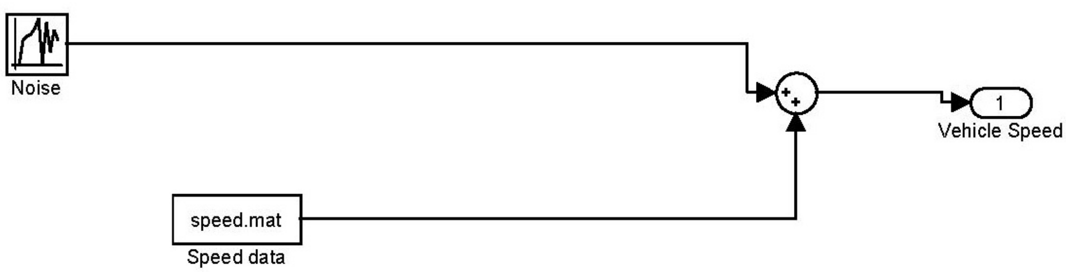

Figure A-5: Vehicle Speed Input

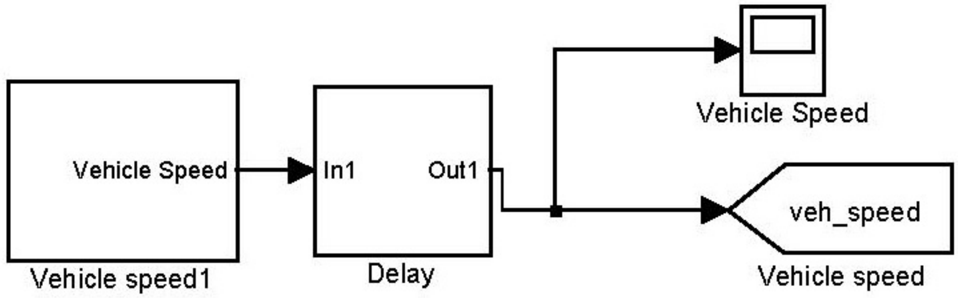

Figure A-6: Vehicle Speed Input Sent to Global From-Block

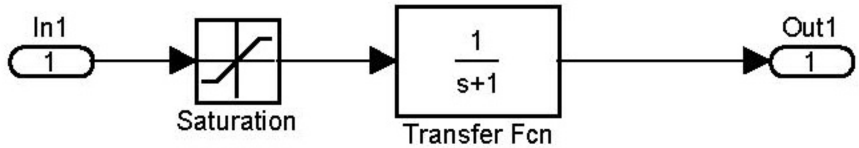

Figure A-7: Convert Vehicle Speed from a Ramp to a Smooth Curve

Figures A-8 and A-9 show how the steering angle of the vehicle is read from a data file and made available to the entire system.

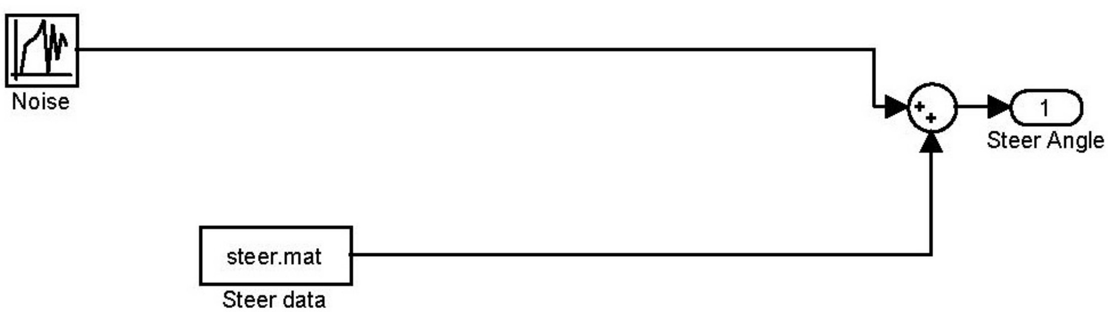

Figure A-8: Steering Input

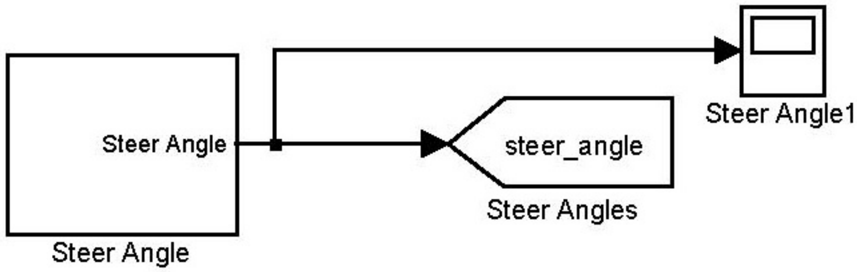

Figure A-9: Steering Input Sent to Global From-Block

Figure A-10 is the central control and simulation of the model. The first part of the system takes in various values as its input and the second part simulates its effect on a real vehicle-trailer system. Figure A-11 shows a simple delay block that delays the response of the slider so that it doesn't move to the commanded position instantaneously. This makes the simulation more realistic.

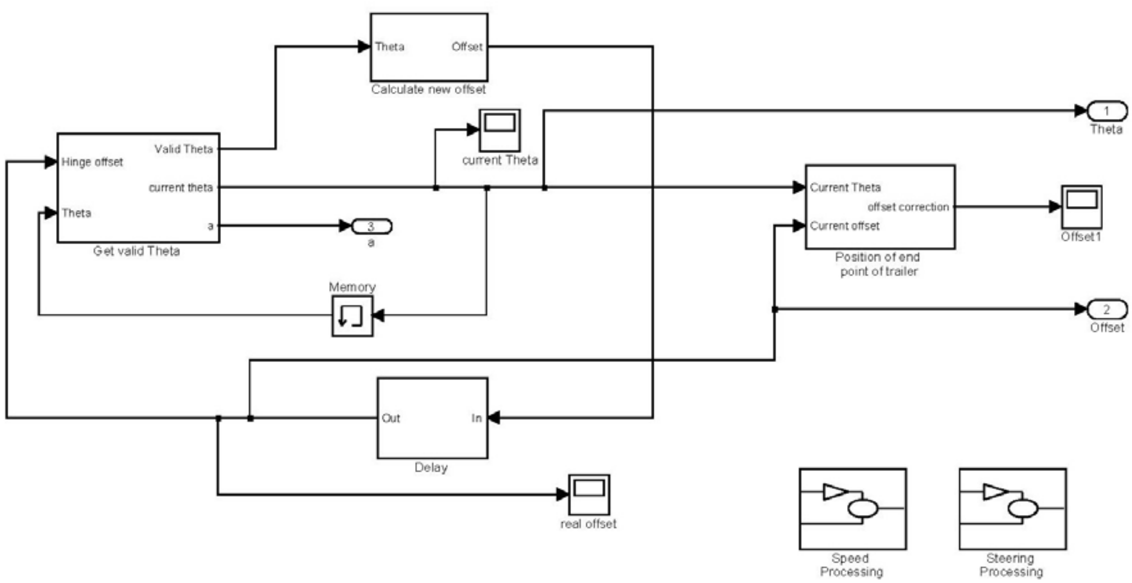

Figure A-10: Central Control of Model

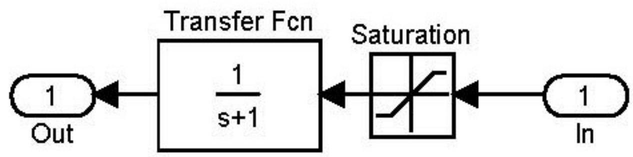

Figure A-11: A Delay Function to Make the Model Realistic

In a real system the value of Theta would be simply read off a sensor but in the case of a software model this has to be simulated as shown in Figure A-12. Besides this the required Theta to make the system stable is also required and this is calculated as shown in Figures A-12, A-13, A-14 and A-15.

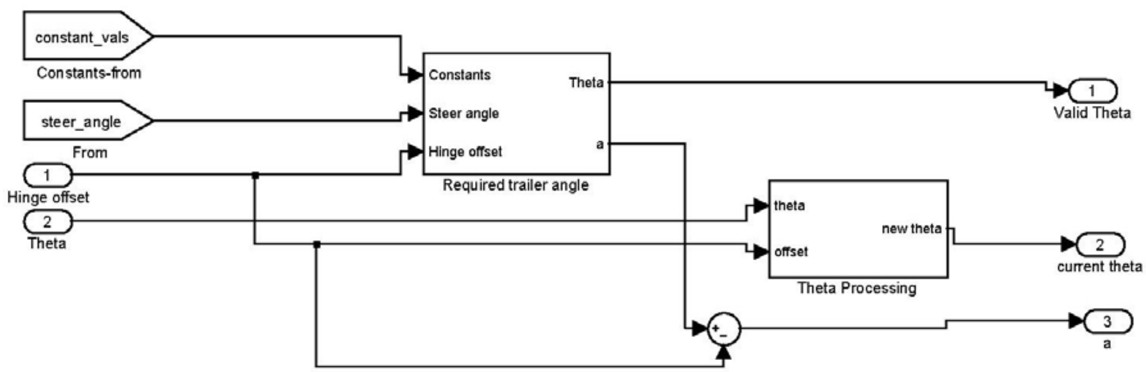

Figure A-12: Current Theta Processing

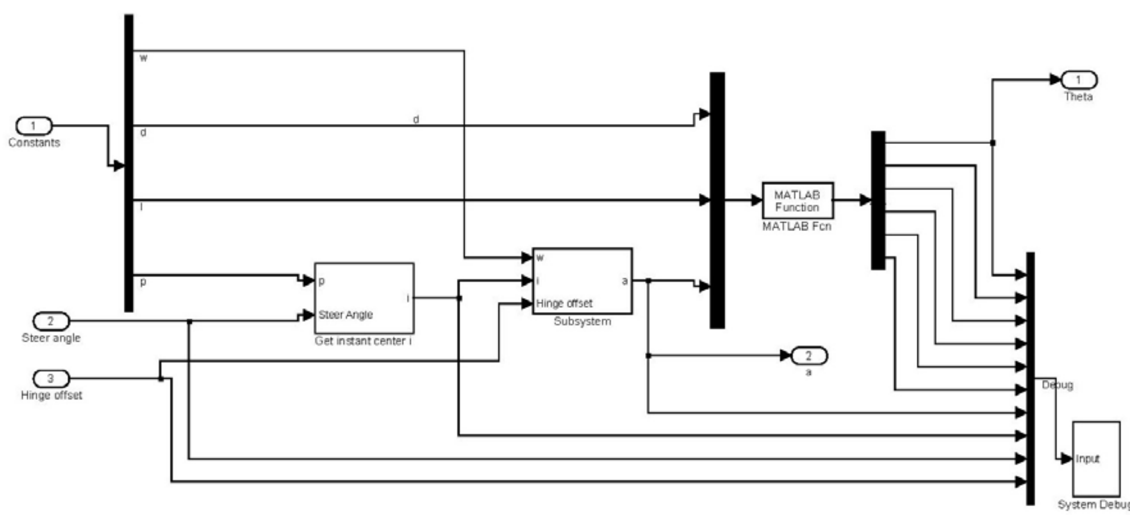

Figure A-13: Required Theta Processing

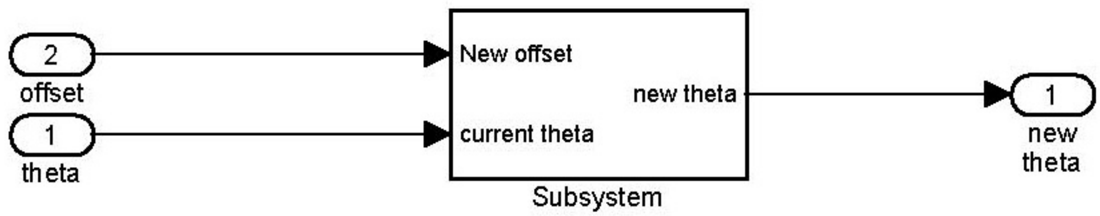

Figure A-14: Calculation of New Required Theta – I

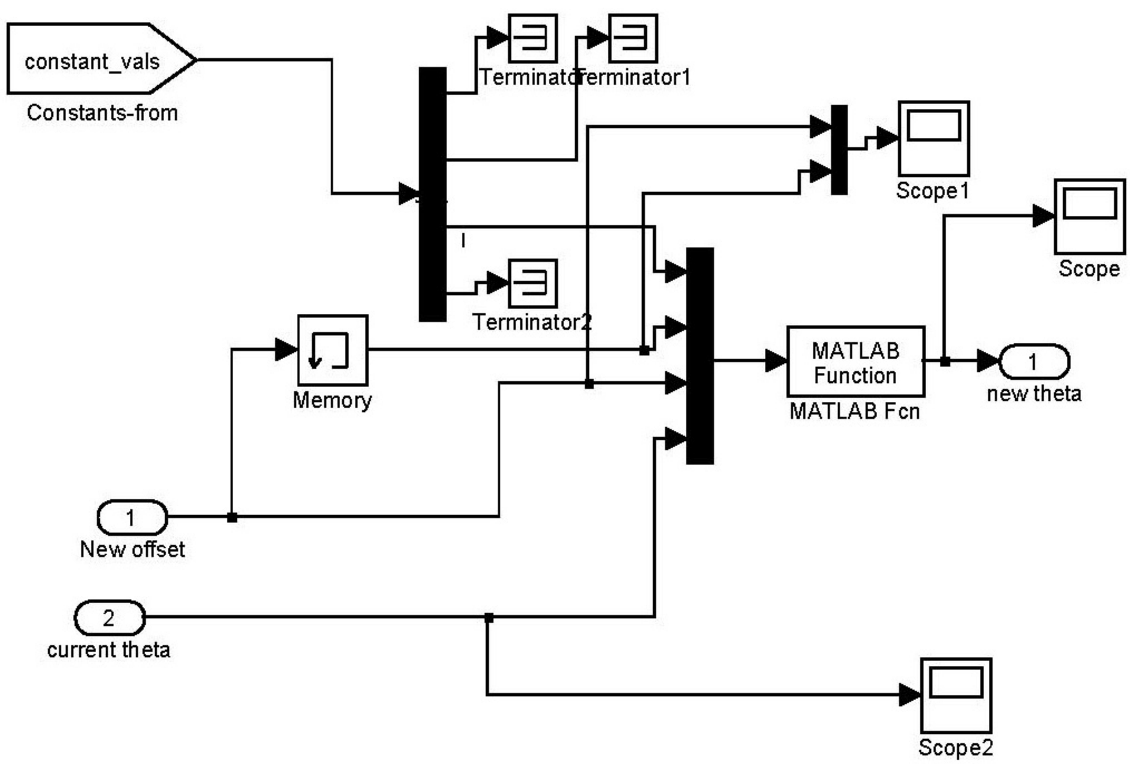

Figure A-15: Calculation of New Required Theta – II

For the system to run other values have to be calculated as illustrated in the figures below. Figure A-16 shows how the distance of the instant center from the rear wheel is calculated. Figure A-17 shows how the turning radius of the vehicle is calculated.

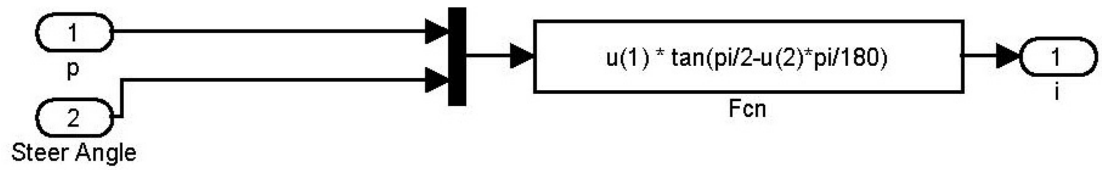

Figure A-16: Calculation of i (Distance of the Instant Center from the Rear Wheel)

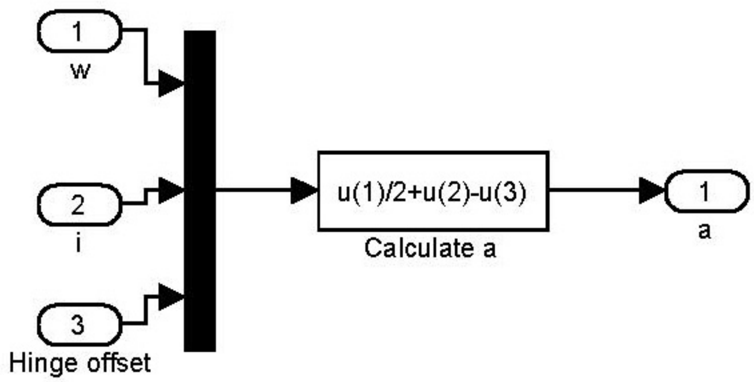

Figure A-17: Calculation of a, the Turning Radius

After the required Theta is calculated, the offset required to change the trailer angle is calculated as shown in Figures A-18, A-19 and A-20.

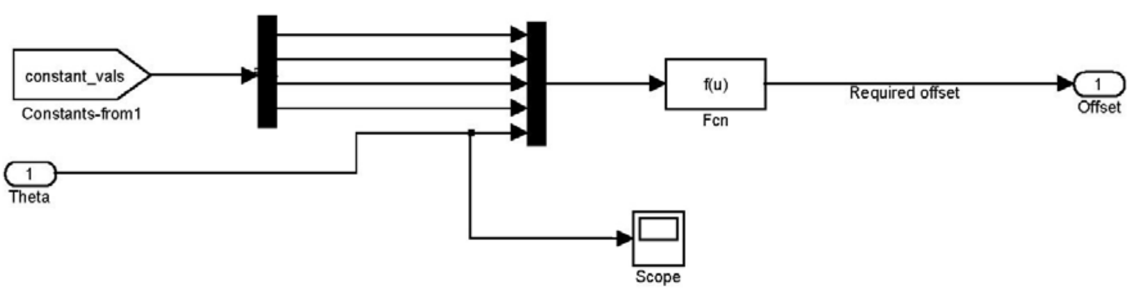

Figure A-18: Calculation of Required Offset

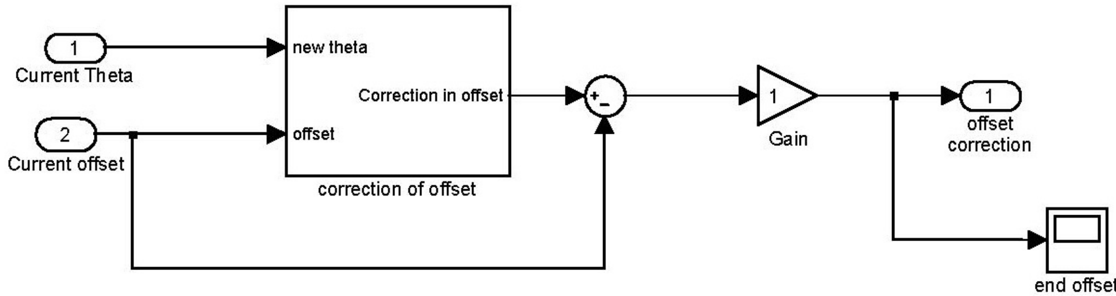

Figure A-19: Calculation of the Correction in Offset Required - I

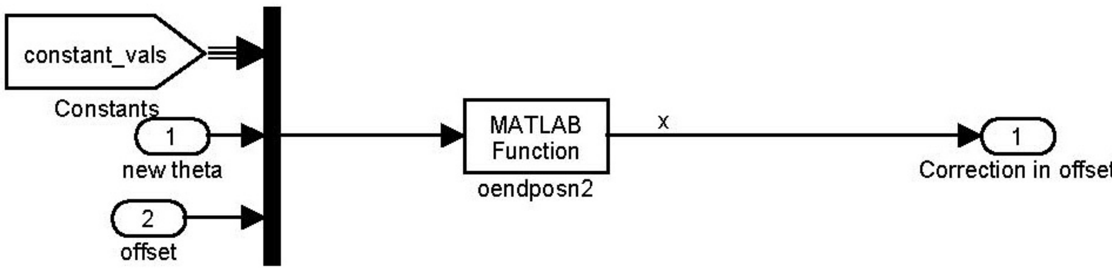

Figure A-20: Calculation of the Correction in the Offset Required – II

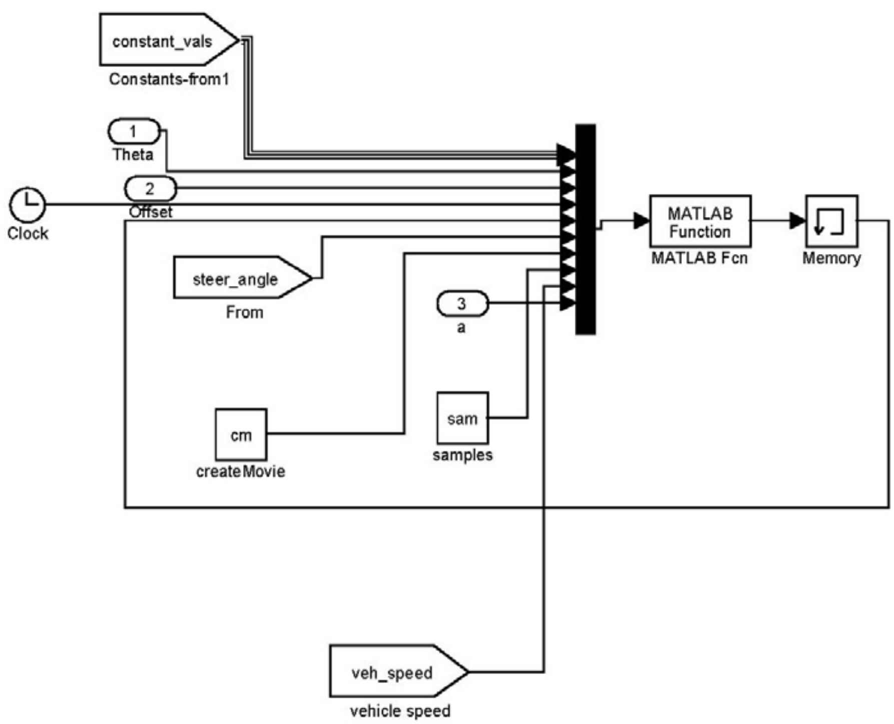

Figure A-21: Animation of Model

These values are fed back into the system and the whole cycle starts again for the next time step.

Figure A-21 shows the values that are fed into the animation system for the model.

Figure A-22 helps output all values to graphs for debugging as well as for plotting outputs.

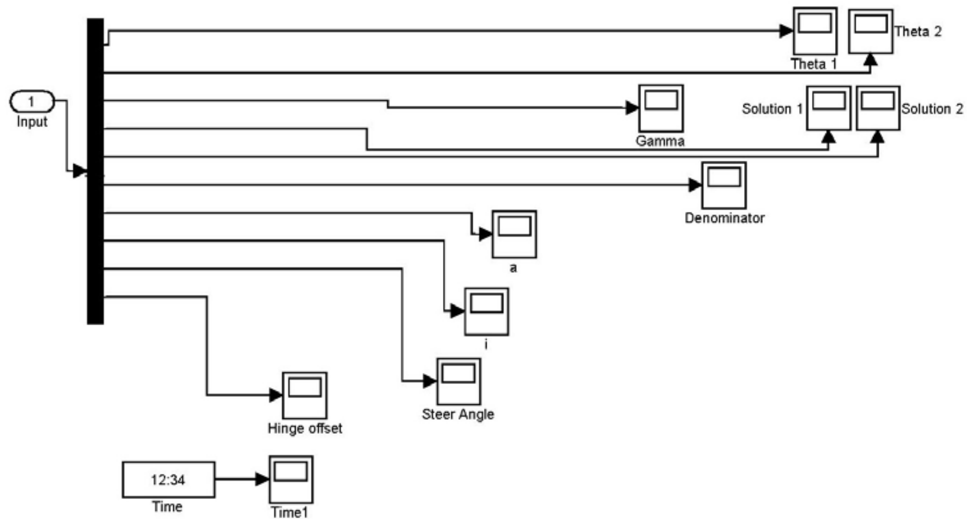

Figure A-22: Debug Box for Troubleshooting and viewing outputs

LIST OF REFERENCES

1. Tesar, D. and Matthew, G., “A New Coupling Hitch for Car-Trailer Combinations which Eliminates Swaying,” Society of Automotive Engineers SP-80/463, 1980.

2. P. Ferbach., “A Method of Progressive Constraints for Nonholonomic Motion Planning,” IEEE Transactions on Robotics and Automation, 14(1):172-179, 1998.

3. J.P. Laumond, F. Lamiraux and S. Sekhavat, “Guidelines in Nonholonomic Motion Planning in Robot Motion Planning and Control,” Lectures Notes in Control and Information Sciences, Springer Verlag, 343p, 1998.

4. Dean F. Hougen, John Fischer, Maria Gini, and James Slagle, “Fast Connectionist Learning for Trailer Backing Using a Real Robot,” In IEEE Int'l Conf. on Robotics and Automation, pp. 1917-1922, 1996.

5. F. Lamiraux, S. Sekhavat, and J.-P. Laumond, “Motion Planning and Control for Hilare Pulling a Trailer,” IEEE Trans. Robotics and Automation, 15(4):640-652, August 1999.

6. M. Vendittelli, G. Oriolo, and J.-P. Laumond, “Steering Nonholonomic Systems via Nilpotent Approximations: The General Two-Trailer System,” 1999 IEEE Int. Conf. on Robotics and Automation, pp. 823-829, 1999.

7. P. Svestka and J. Vleugels, “Exact Motion Planning for Tractor-Trailer Robots,” In Proc. IEEE Internat. Conf. on Robotics and Automation, pp. 2445-2450, Nagoya, Japan, 1995.

8. R. H. Kwong, “Mathematical Modeling of a Physical System: Inverted Pendulum,” Available from URL: http://www.control.utoronto.ca/people/profs/kwong/ece356/notes-ch1.ps. Accessed in 05/2003.

9. “CTM Example: Inverted Pendulum Modeling,” Available at URL: http://www.engin.umich.edu/group/ctm/examples/pend/invpen.html. Accessed in 05/2003.

10. P. Choudhury and K. M. Lynch, “Rolling Manipulation with a Single Control,” Conference on Control Applications, Mexico City, Mexico, September 2001.

11. A. Marigo and A. Bicchi, "Rolling Bodies with Regular Surface: Controllability Theory and Applications," Submitted to IEEE Trans. Robotics and Automation, 1998.

12. C. Crane, J. Duffy, Kinematic Analysis of Robot Manipulators, Cambridge University Press, May 1998.

13. Coutinho, Murilo G., Dynamic Simulations of Multibody Systems, New York: Springer, 2001.

14. Meriam, J. L. (James L.), Engineering Mechanics, New York: Wiley, 1978.

15. McGill, David J., Engineering Mechanics: an Introduction to Dynamics, 2nd ed., Boston, Mass.: PWS -Kent Pub. Co., 1989.

16. Prentis, James Martin., Engineering Mechanics, Oxford: Clarendon Press; New York: Oxford University Press, 1979.

17. Shabana, Ahmed A., Dynamics of Multibody Systems, New York: Wiley, 1989.

18. Hibbeler, R. C., Engineering Mechanics-Dynamics, 4th ed., New York: Macmillan Pub. Co.; London: Collier Macmillan Publishers, 1986.

19. J. A. Sellers, "Section 1. Why Taylor Series," Available at URL: http://www.krellinst.org/UCES/archive/resources/taylor_series/node1.shtml, Accessed in 08/2003.

BIOGRAPHICAL SKETCH

Amit David Jayakaran was born on May 1st, 1979, in India. He received this Bachelor of Engineering in mechanical engineering from the College of Engineering, Anna University, in India in April 2001.

He joined the University of Florida for his master's in mechanical engineering. He has been a research assistant working on enhanced trailer backing with the Mechanical and Aerospace Engineering Department at the University of Florida. His research interests include controls, robotics and industrial automation.